

Spectroscopic survey of LAMOST

Yongheng Zhao
(National Astronomical Observatories of China)

On behalf of the LAMOST operation team

Outline

- **LAMOST**
- **Spectroscopic Survey of LAMOST**
- **LAMOST Sciences**

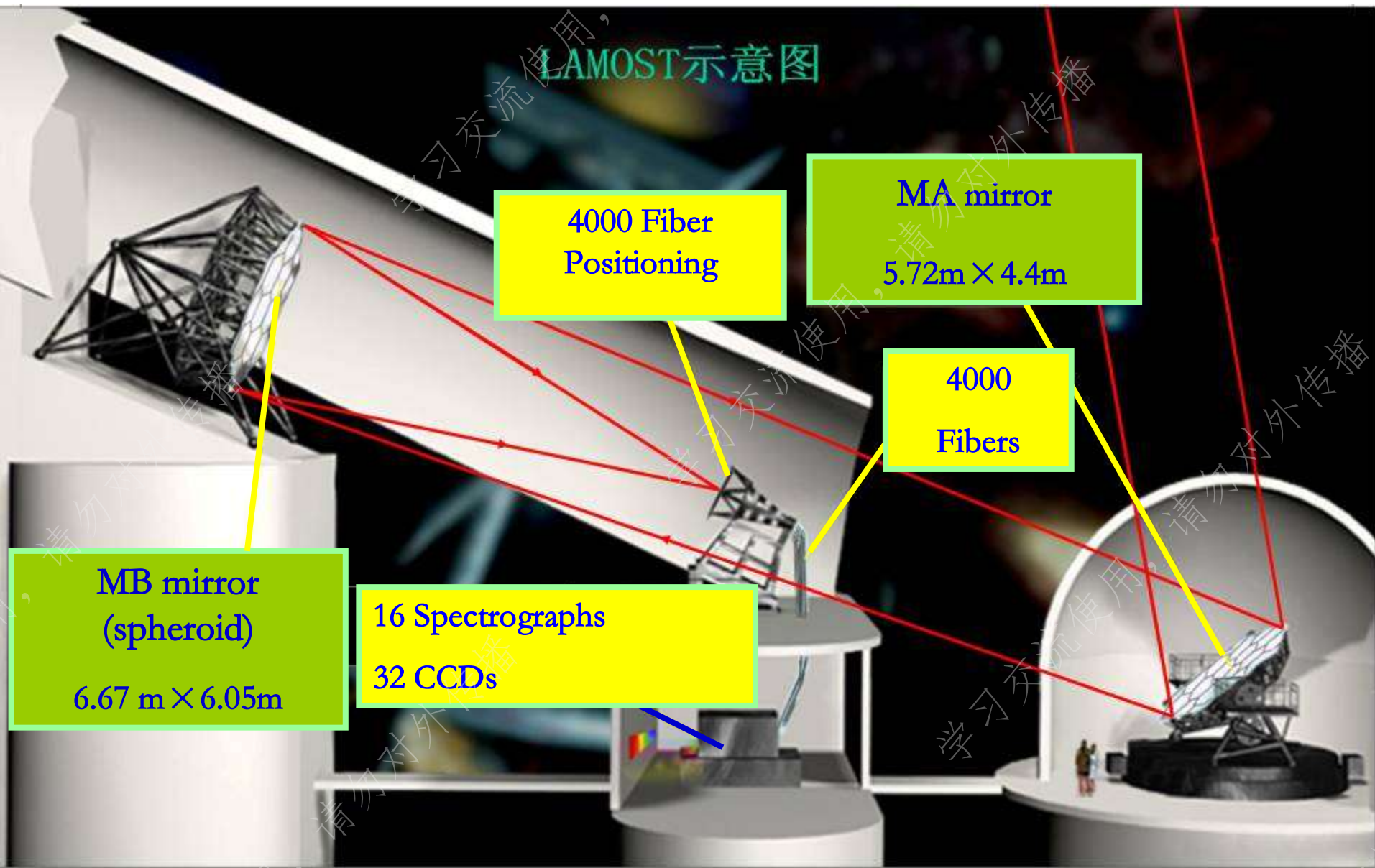


LAMOST – A unique survey telescope



Structure of LAMOST

LAMOST示意图



Innovations in LAMOST

a active reflecting Schmidt telescope

the Wang-Su type telescope which could get the **largest aperture for wide field of view**

large field of view (5 deg) +large aperture (4m)

achieved by new type of active optics — **thin deformable segmented mirrors active optics**

4000 optical fibers on focal surface

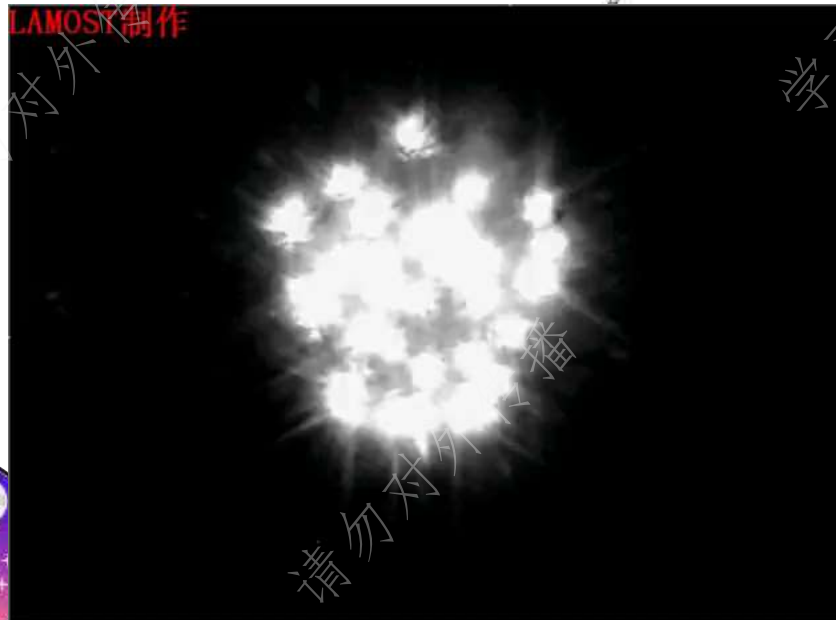
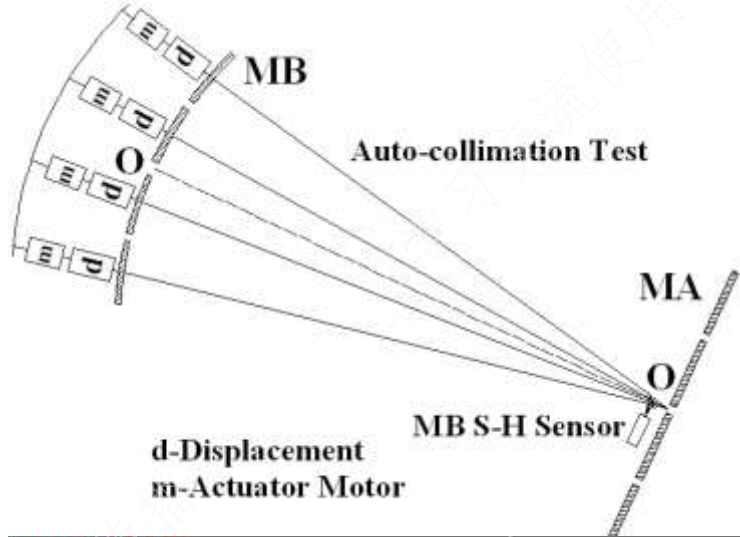
Parallel controllable fiber positioning opened the way to take **thousands optical fibers** observing in short time



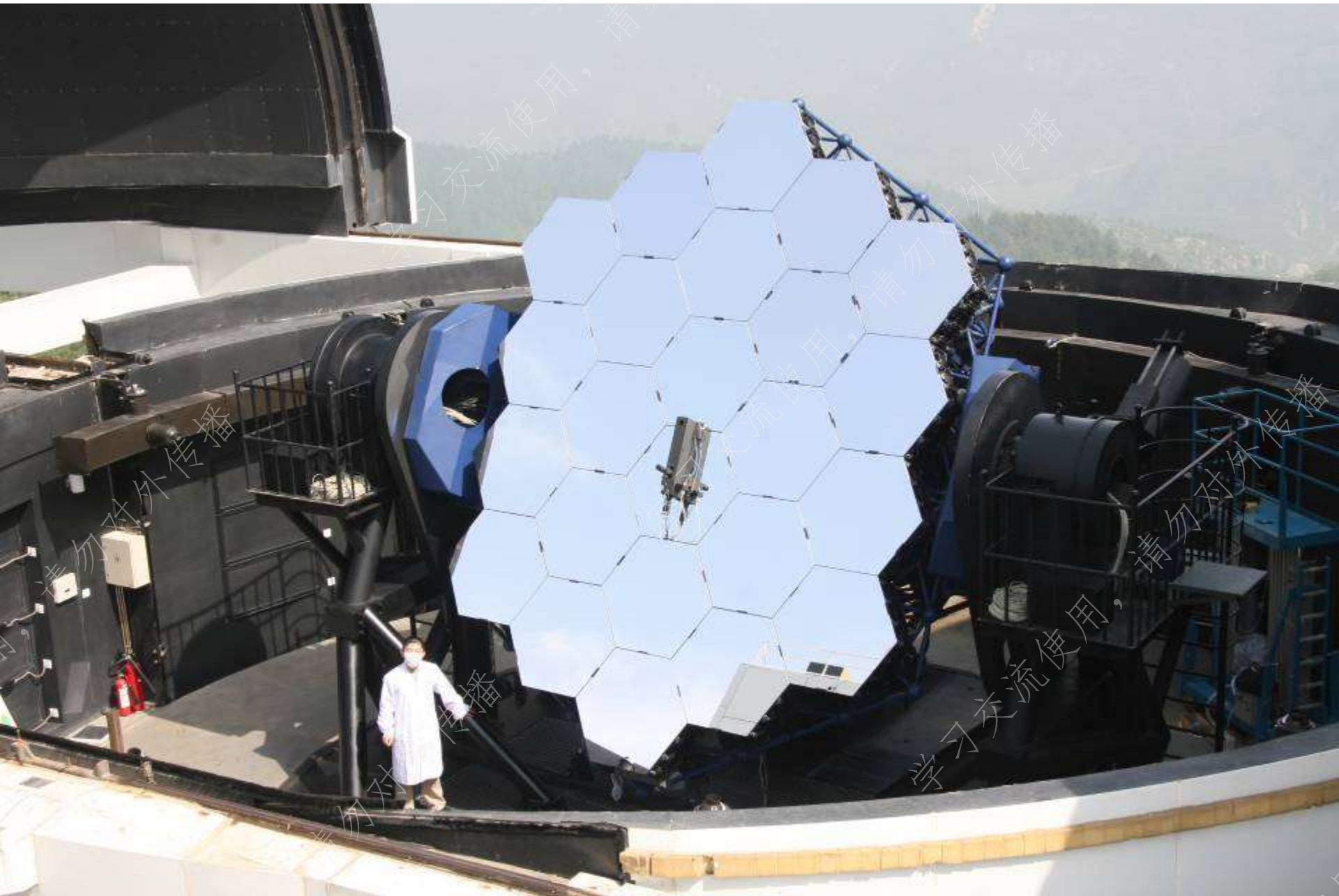
MB: 37 sub-mirrors (6.67m x 6.05m)



- Active optics for segmented 37 MB sub-mirrors

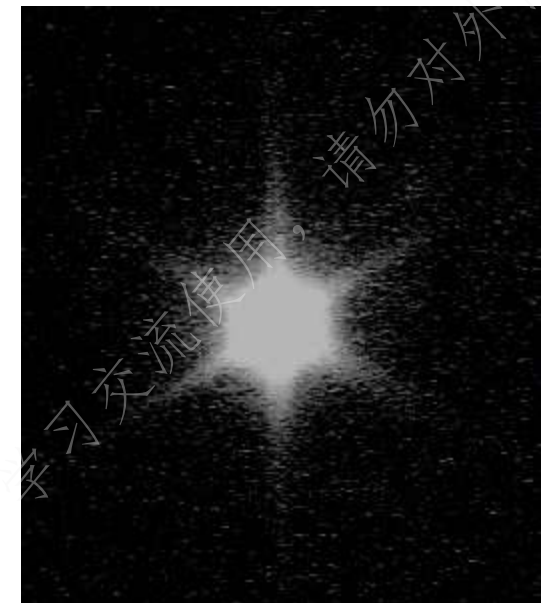
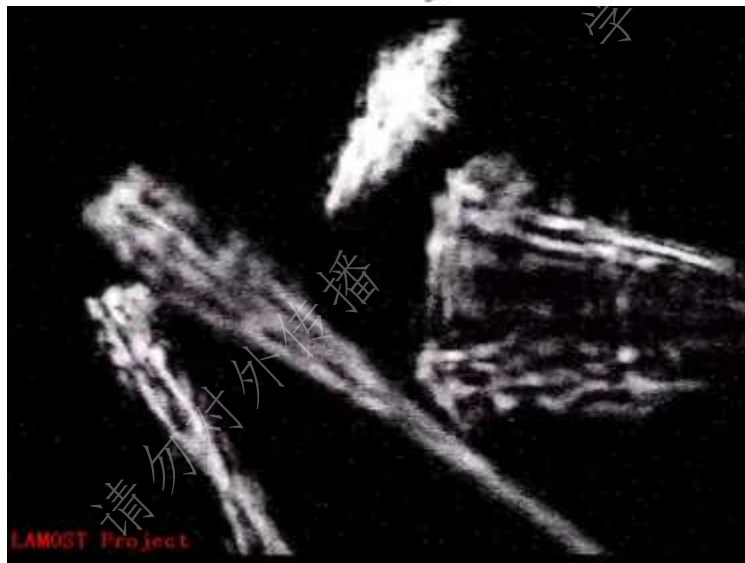
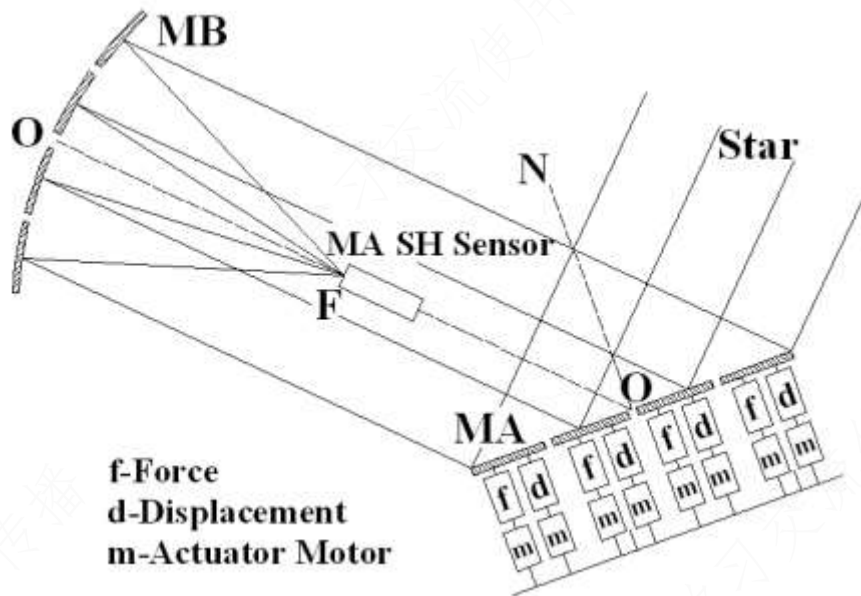


MA: 24 sub-mirrors (5.72m x 4.4m)



Active reflecting Schmidt optical system

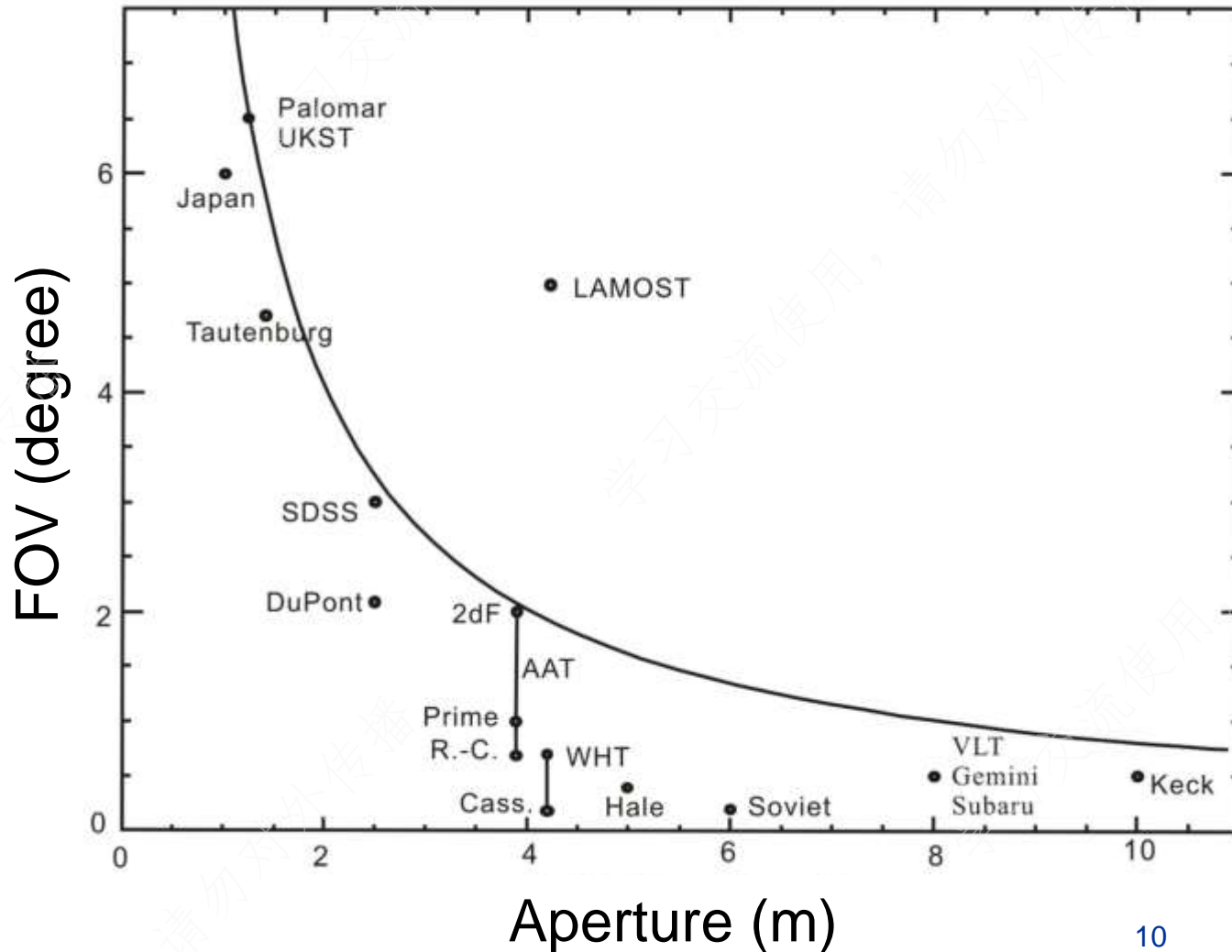
Ma (24 sub-mirrors) + Mb (37 sub-mirrors)



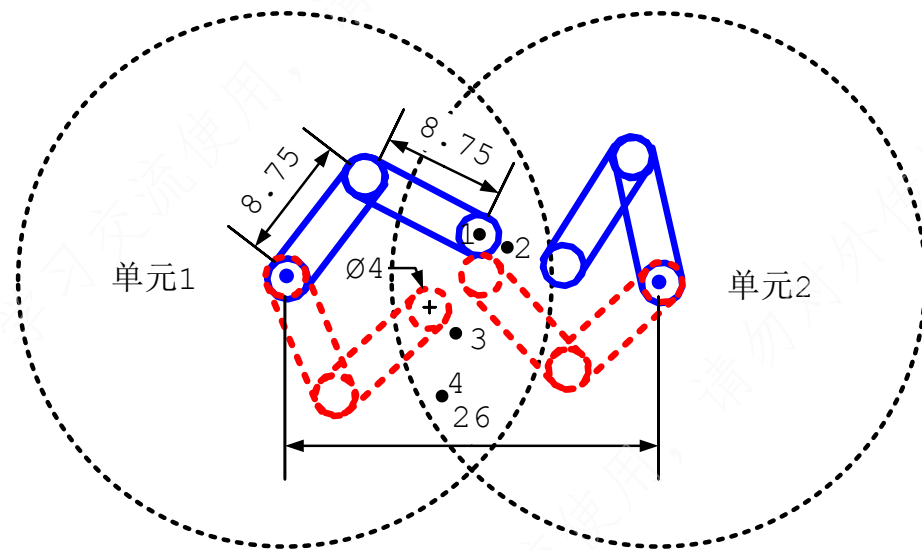
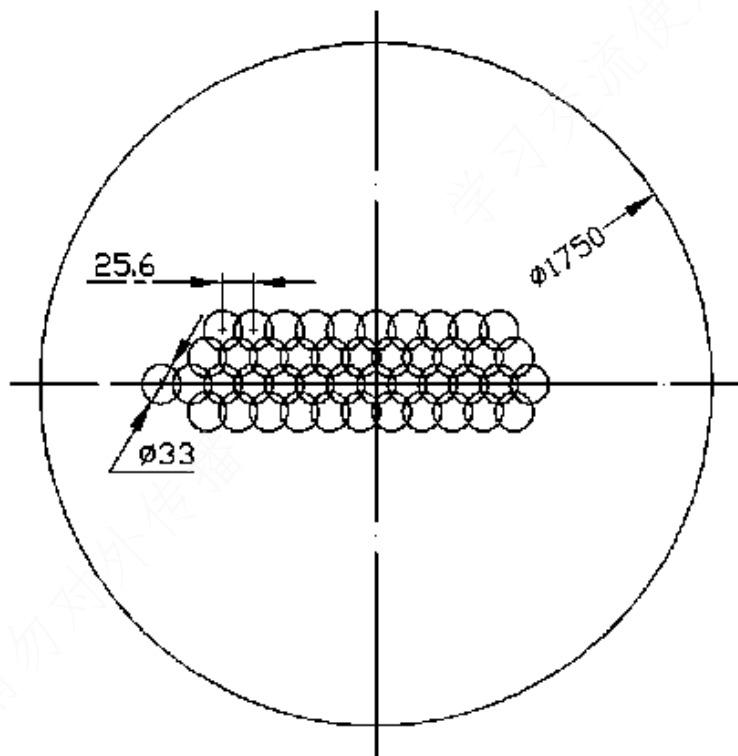
Aperture – field of view

(prof. Wiltrop in Cambridge University)

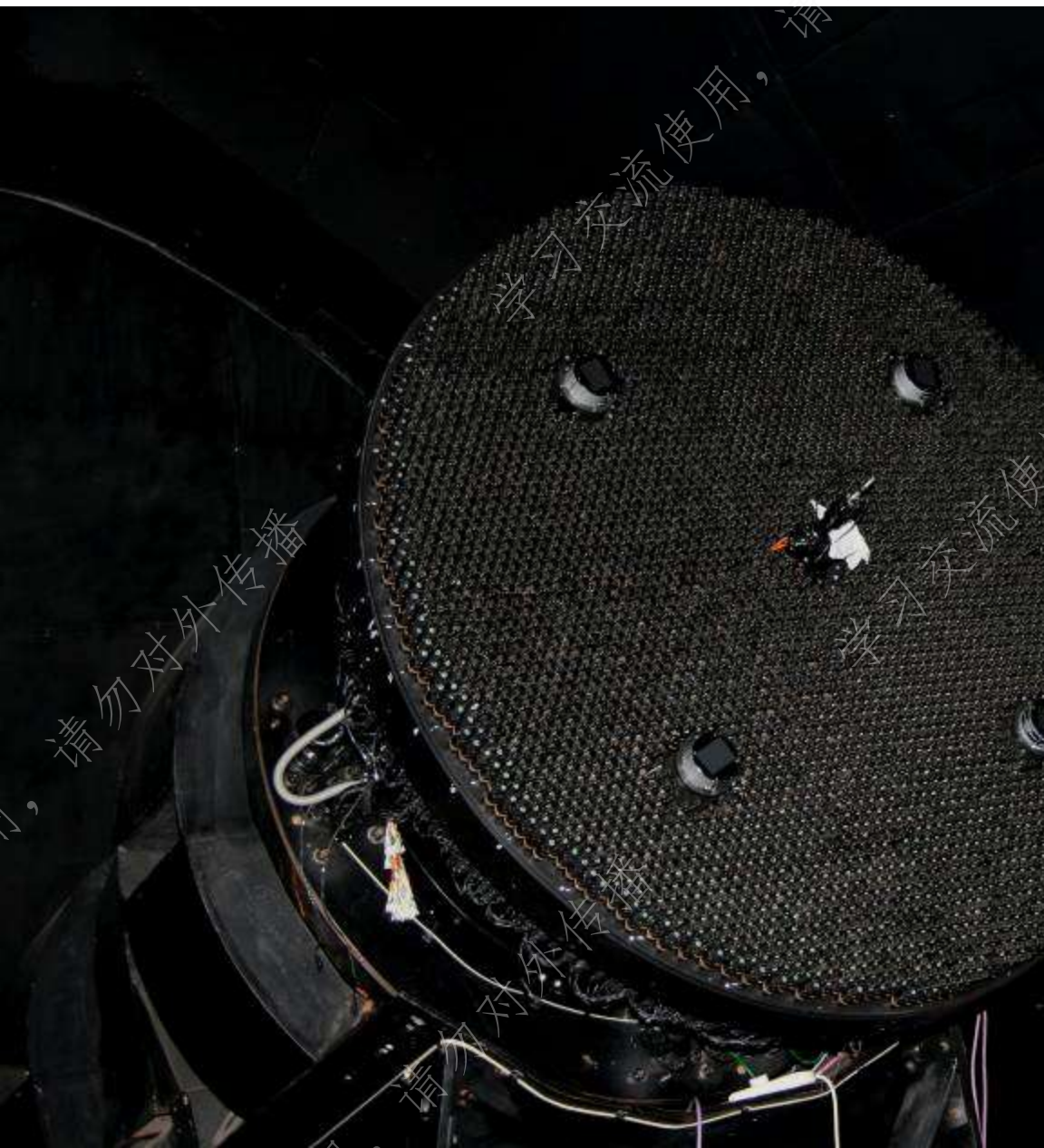
《Astronomical Optics and Elasticity Theory》, 2009, p. 41



New technique: Parallel controllable fiber positioning



4000 fiber positioning units



并行可控式光纤定位单元

New spectroscopical survey projects

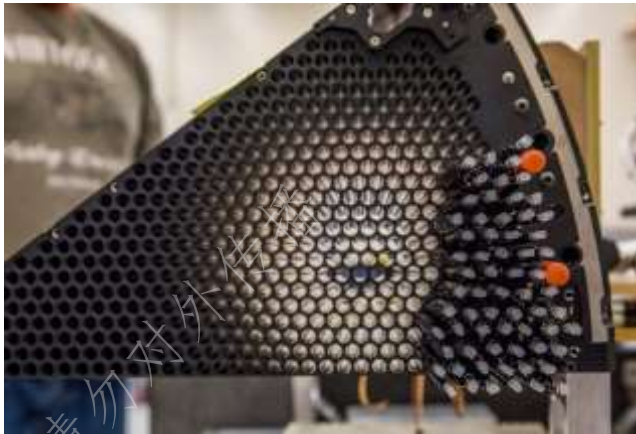


Figure 3.10-1. Positioner Bench Populated with One Module and a Single Positioner

SDSS-V: New hardware
✓ FPS (Focal Plane System)

SDSS-V
Focal Plane System Overview



Richard Pogge
The Ohio State University

DESI (USA)

SUBARU / PFS (Japan)

SDSS-V (USA)



Great Paris Exhibition Telescope

(lens at the same scale)
Paris, France (1900)

Yerkes Observatory

(40" refractor lens at the same scale)
Williams Bay, Wisconsin (1893)

Hooker (100")

Mt Wilson, California (1917)

Hale (200")

Mt Palomar, California (1948)

Multi Mirror Telescope

(1979-1998) Mount Hopkins, Arizona

Hobby-Eberly Telescope

(1999-) Davis Mountains, Texas (1996)

BTA-6 (Large Altazimuth Telescope)

Zelenchuksky, Russia (1975)

Large Zenith Telescope

British Columbia, Canada (2003)

Gaia

Earth-Sun L2 point (2014)

Kepler

Earth-trailing solar orbit (2009)

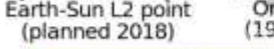
James Webb Space Telescope

Earth-Sun L2 point (planned 2018)

Hubble Space Telescope

Low Earth Orbit (1990)

Tennis court at the same scale



Magellan Telescopes

Las Campanas, Chile (2000/2002)

Overwhelmingly Large Telescope (cancelled)

Arecibo radio telescope at the same scale



Large Sky Area Multi-Object Fiber Spectroscopic Telescope

Hebei, China (2009)

Gran Telescopio Canarias

La Palma, Canary Islands, Spain (2007)

Southern African Large Telescope

Sutherland, South Africa (2005)

Gemini North

Mauna Kea, Hawaii (1999)

Gemini South

Cerro Pachón, Chile (2000)

Large Binocular Telescope

Mount Graham, Arizona (2005)

Very Large Telescope

Cerro Paranal, Chile (1998-2000)

Magellan Telescopes

Las Campanas, Chile (2000/2002)

Giant Magellan Telescope

Las Campanas Observatory, Chile (planned 2020)

Keck Telescope

Mauna Kea, Hawaii (1993/1996)

Subaru Telescope

Mauna Kea, Hawaii (1999)

Thirty Meter Telescope

Mauna Kea, Hawaii (planned 2022)



Keck Telescope

Mauna Kea, Hawaii (1993/1996)

Subaru Telescope

Mauna Kea, Hawaii (1999)

Thirty Meter Telescope

Mauna Kea, Hawaii (planned 2022)

Gemini North

Mauna Kea, Hawaii (1999)

Gemini South

Cerro Pachón, Chile (2000)

Large Binocular Telescope

Mount Graham, Arizona (2005)

Large Synoptic Survey Telescope

El Peñón, Chile (planned 2020)

Very Large Telescope

Cerro Paranal, Chile (1998-2000)

Magellan Telescopes

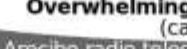
Las Campanas, Chile (2000/2002)

Giant Magellan Telescope

Las Campanas Observatory, Chile (planned 2020)

Overwhelmingly Large Telescope (cancelled)

Arecibo radio telescope at the same scale



Basketball court at the same scale

Keck Telescope

Mauna Kea, Hawaii (1993/1996)

Subaru Telescope

Mauna Kea, Hawaii (1999)

Thirty Meter Telescope

Mauna Kea, Hawaii (planned 2022)

Gemini North

Mauna Kea, Hawaii (1999)

Gemini South

Cerro Pachón, Chile (2000)

Large Binocular Telescope

Mount Graham, Arizona (2005)

Large Synoptic Survey Telescope

El Peñón, Chile (planned 2020)

Very Large Telescope

Cerro Paranal, Chile (1998-2000)

Magellan Telescopes

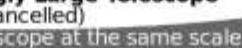
Las Campanas, Chile (2000/2002)

Giant Magellan Telescope

Las Campanas Observatory, Chile (planned 2020)

Overwhelmingly Large Telescope (cancelled)

Arecibo radio telescope at the same scale

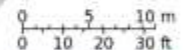


Basketball court at the same scale

European Extremely Large Telescope

Cerro Armazones, Chile (planned 2022)

Human at the same scale



Basketball court at the same scale



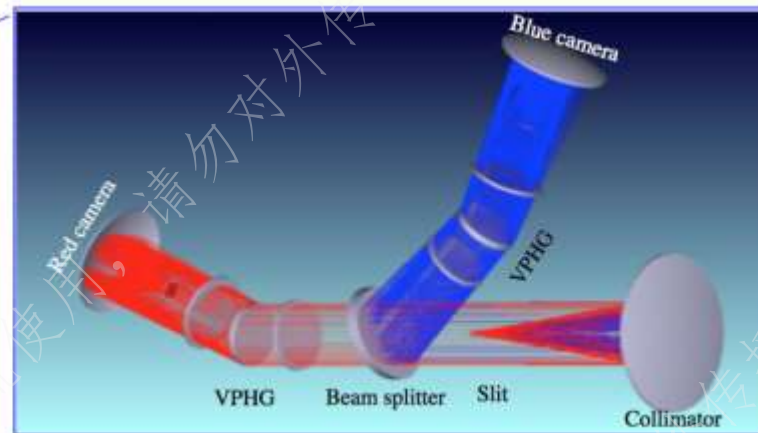
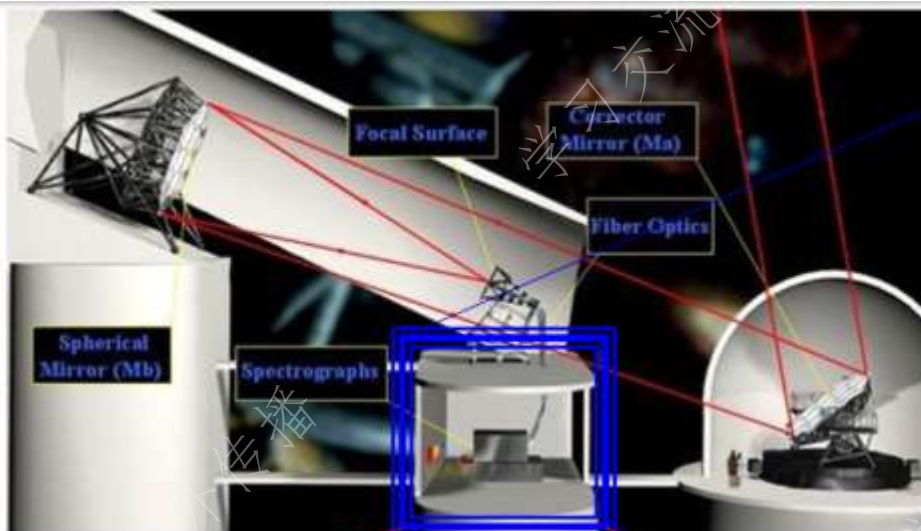
Spectroscopic Survey of LAMOST

| | | low resolution mode | medium resolution mode |
|-----------------------|---------|---------------------------|---------------------------|
| Sep. 2011 – Jun. 2012 | 1 year | pilot survey | |
| Sep. 2012 – Jun. 2017 | 5 years | 1st regular survey | |
| Sep. 2017 – Jun. 2018 | 1 year | continue | test survey |
| Sep. 2018 – Jun. 2023 | 5 years | 2nd regular survey | 2nd regular survey |

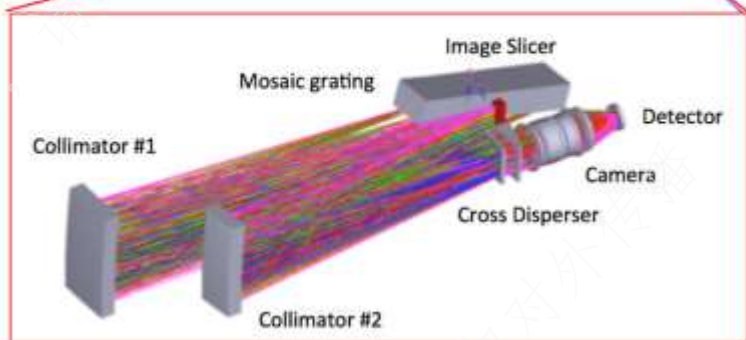
- **Scientific goals:**
 - **Structure & evolution of the Milky Way**
 - **Stellar astrophysics**
 - **Quasars & galaxies**



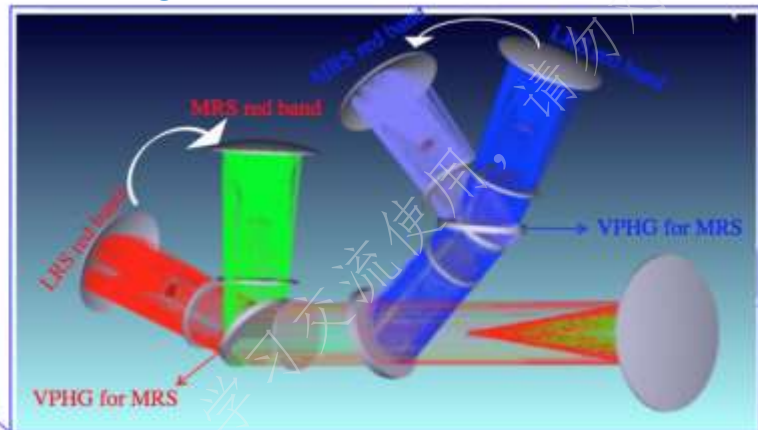
low & medium resolution modes



16 spectrographs in low-resolution mode



1 spectrographs in high-resolution mode



16 spectrographs in medium-resolution mode

Medium-resolution survey (MRS)

- Accuracy: $V_r < 1\text{km/s}$
- ~ 20 elements abundances
 - Li, C, Na, Mg, Si, Ca, Sc, Ti, V, Cr, Mn, Fe, Co, Ni, Cu, Y, Sm, Nd and Ba etc.
- 4000 fibers
- $g < 15$ Mag.
- $R \sim 7500$

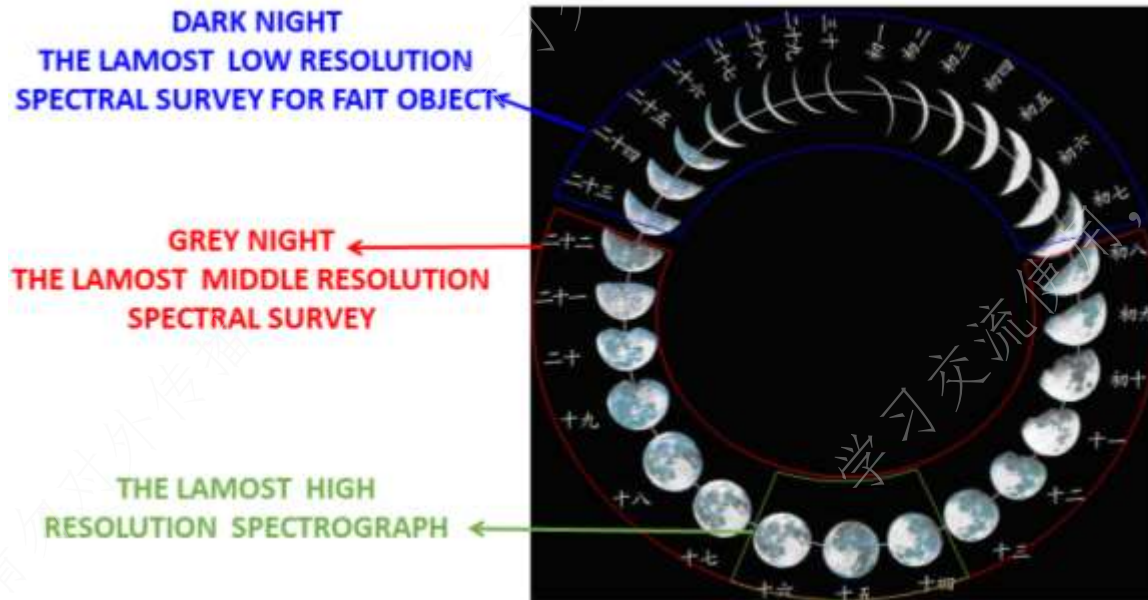
| | $R \sim 1800$ | $R \sim 7500$ |
|------------------|---------------------|---------------------|
| V_r | $\leq 5\text{km/s}$ | $\leq 1\text{km/s}$ |
| T_{eff} | 200k | 100k |
| Log g | 0.2dex | 0.1 dex |
| [Fe/H] | 0.2dex | 0.1 dex |
| [α /Fe] | 0.2dex | 0.1 dex |



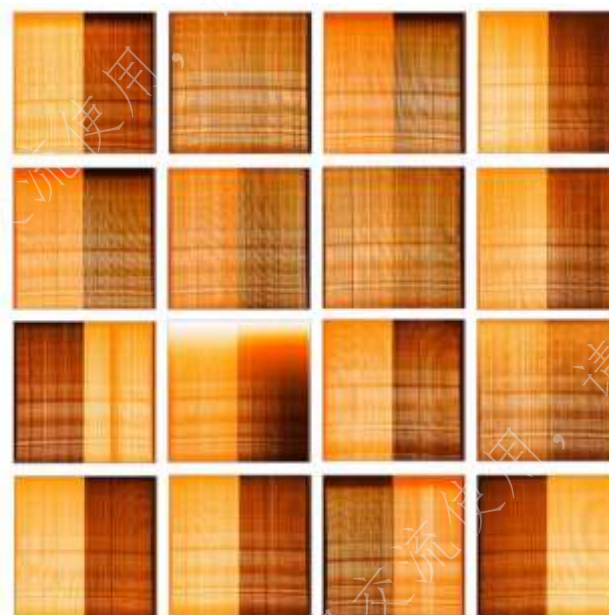
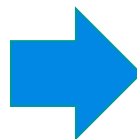
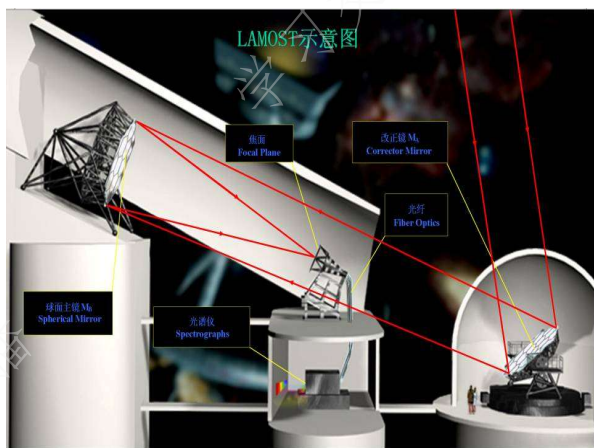
The 2nd regular survey of LAMOST

2018.9 - 2023.6:

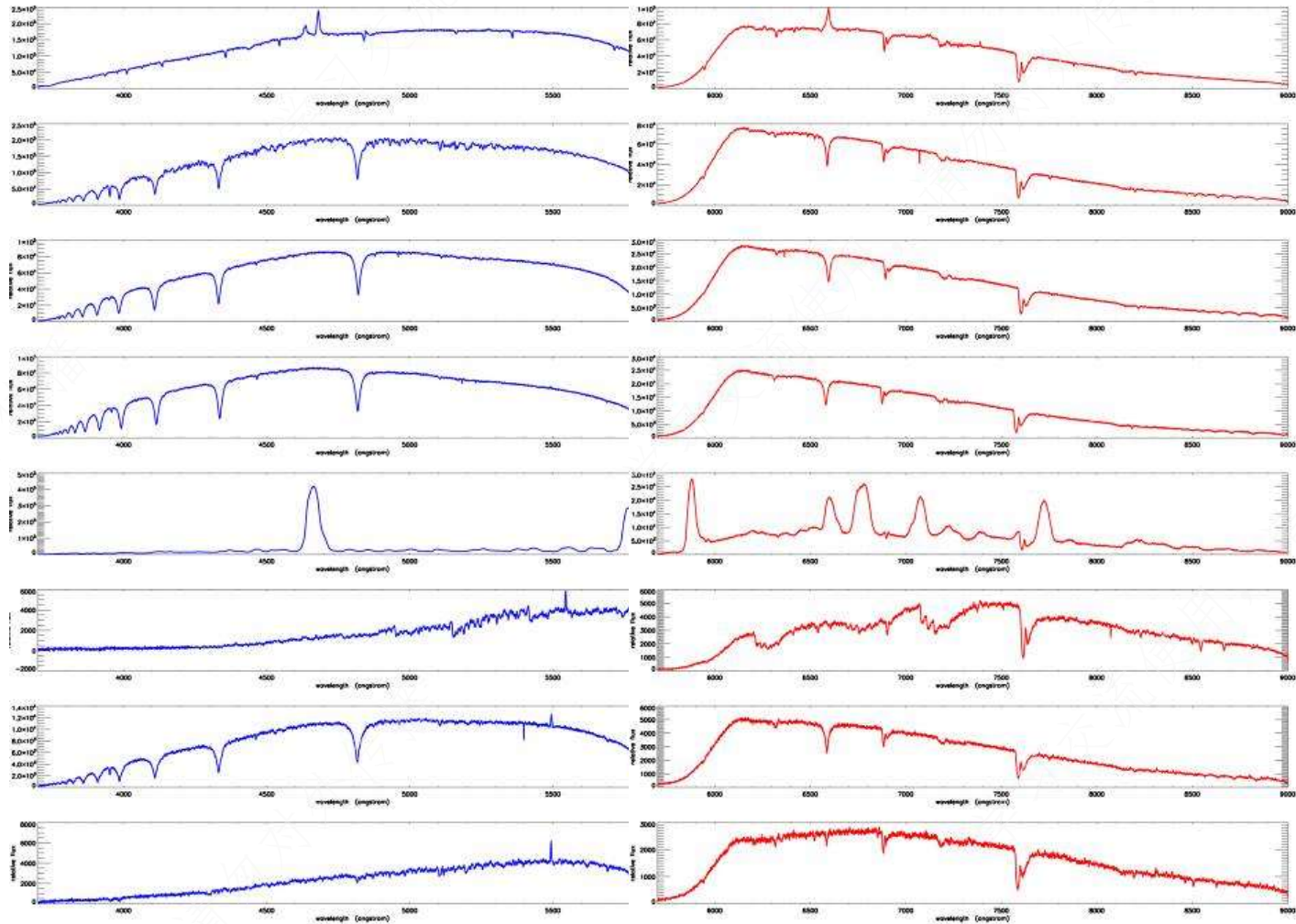
- survey in low-resolution (dark nights)
- survey in median-resolution (bright nights)
- observations in high-resolution (full moon nights)



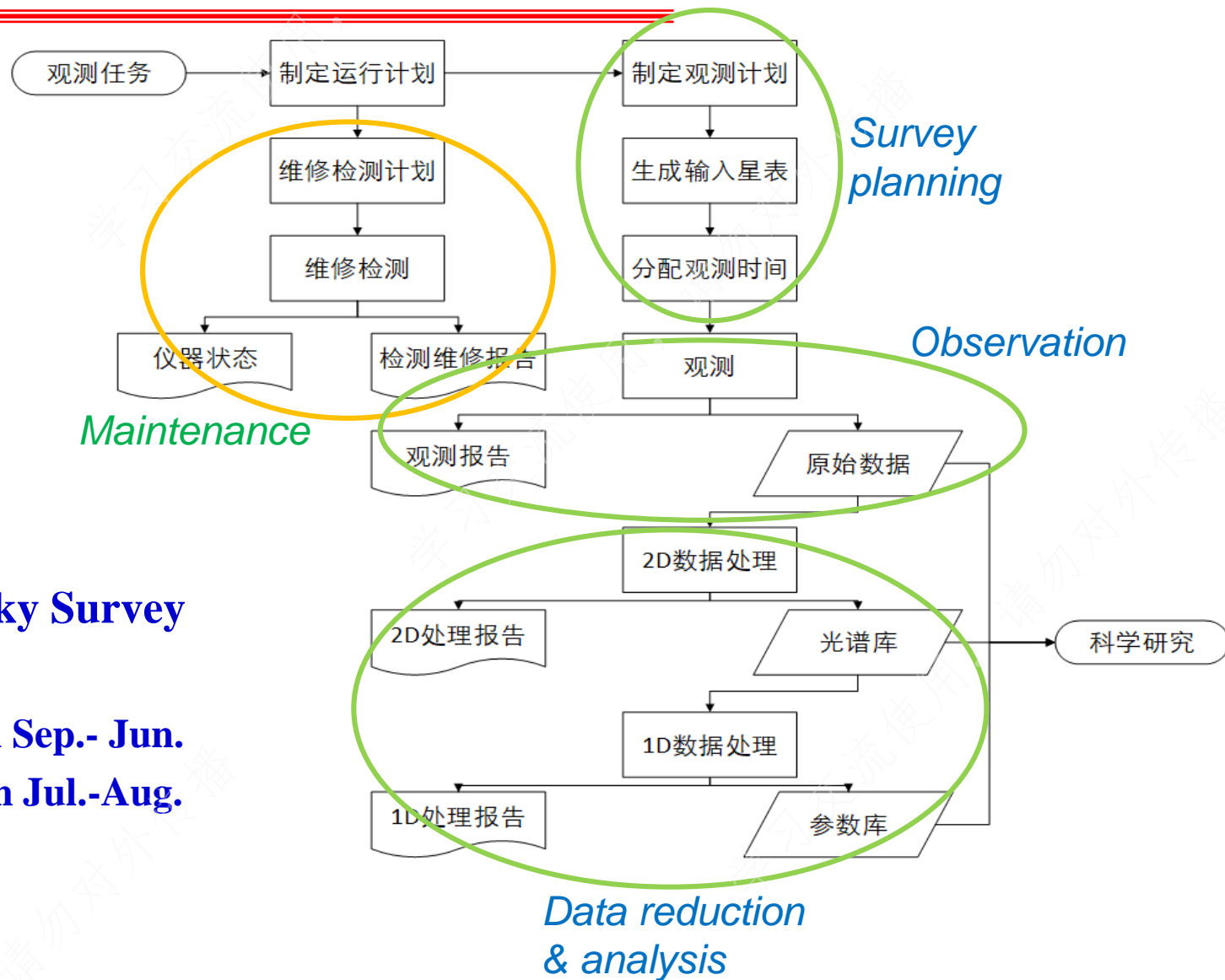
Raw data by LAMOST



Data reduction



Operation of LAMOST



Observation of Sky Survey

- Observation in Sep.- Jun.
- Maintenance in Jul.-Aug.



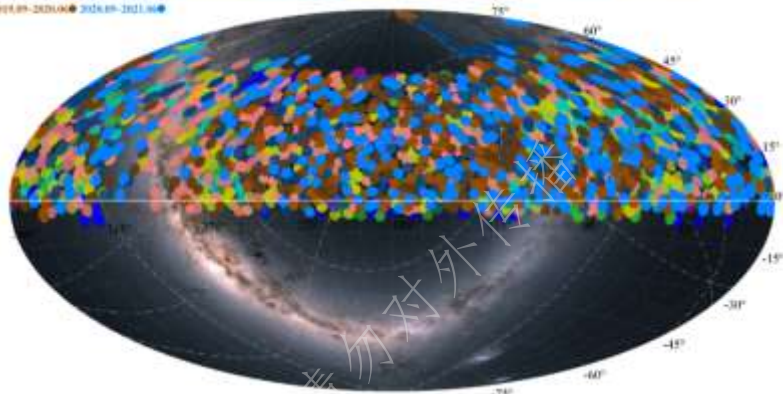
~ 20,000,000 spectra by LAMOST

- DR9 dataset (Mar. 2022)
 - Observed: Sep. 2011 – Jun. 2021

| | Low-resolution data | Medium-resolution non time-domain data | Medium-resolution time-domain data | Total |
|------------------|---------------------|--|------------------------------------|-----------------|
| Total spectra | 11226252 | 1841959 | 6384475 | 19452686 |
| Spectra (S/N>10) | 10109779 | 1194264 | 3662548 | 14966591 |
| Star parameter | 7060436 | 906003 | 771211 | 8737650 |

The LAMOST spectroscopic survey footprint - LRS

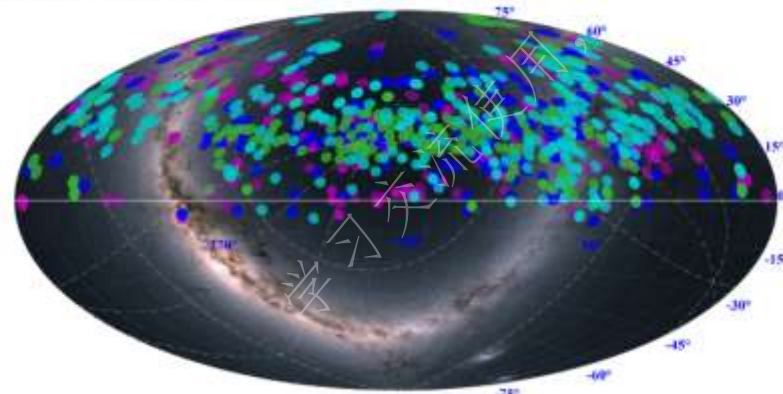
2011.09-2011.06 • 2012.09-2013.06 • 2013.09-2014.06 • 2014.09-2015.06 • 2015.09-2016.06 • 2016.09-2017.06 • 2017.09-2018.06 • 2018.09-2019.06 • 2019.09-2020.06 • 2020.09-2021.06



Low resolution obs. of LAMOST DR9

The LAMOST spectroscopic survey footprint - MRS

before 2018.06 • 2018.09-2019.06 • 2019.09-2020.06 • 2020.09-2021.06



Medium resolution obs. of LAMOST DR9



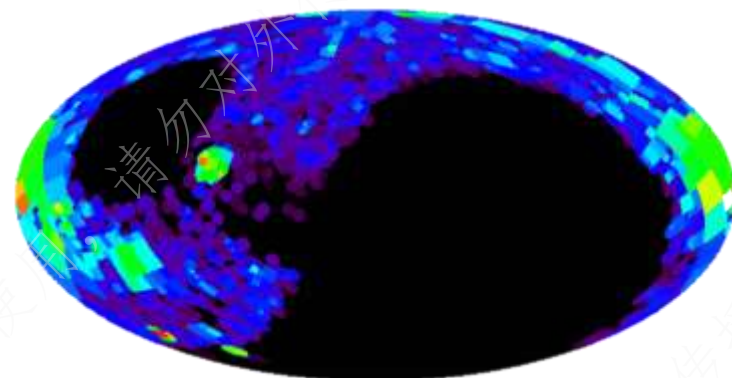
Data release of LAMOST

- **Data police:**
 - **Released to Chinese astronomers and international partners**
 - **Released to Public after 18 months**

| Dataset | Spectra with S/N>10 | Stellar parameters | Data release to domestic / public |
|-------------------------------------|---------------------|--------------------|-----------------------------------|
| Pilot survey (PDR) | 0.55 M | 0.36 M | 2012.08 / 2012.08 |
| Pilot + 1 year Normal survey: (DR1) | 1.74 M | 1.06 M | 2013.09 / 2015.03 |
| Pilot + 2 year Normal survey: (DR2) | 3.27 M | 2.20 M | 2014.12 / 2016.07 |
| Pilot + 3 year Normal survey: (DR3) | 4.66 M | 3.17 M | 2015.12 / 2017.07 |
| Pilot + 4 year Normal survey: (DR4) | 6.21 M | 4.20 M | 2016.12 / 2018.07 |
| Pilot + 5 year Normal survey: (DR5) | 7.77 M | 5.34 M | 2017.12 / 2019.07 |
| Pilot + 6 year Normal survey: (DR6) | 9.37 M | 6.36 M | 2019.03 / 2020.10 |
| Pilot + 7 year Normal survey: (DR7) | 14.48 M | 7.00 M | 2020.03 / 2021.10 |
| Pilot + 8 year Normal survey: (DR8) | 17.23 M | 7.75 M | 2021.03 / 2022.10 |
| Pilot + 9 year Normal survey: (DR9) | 19.45 M | 8.73 M | 2022.03 / 2023.10 |

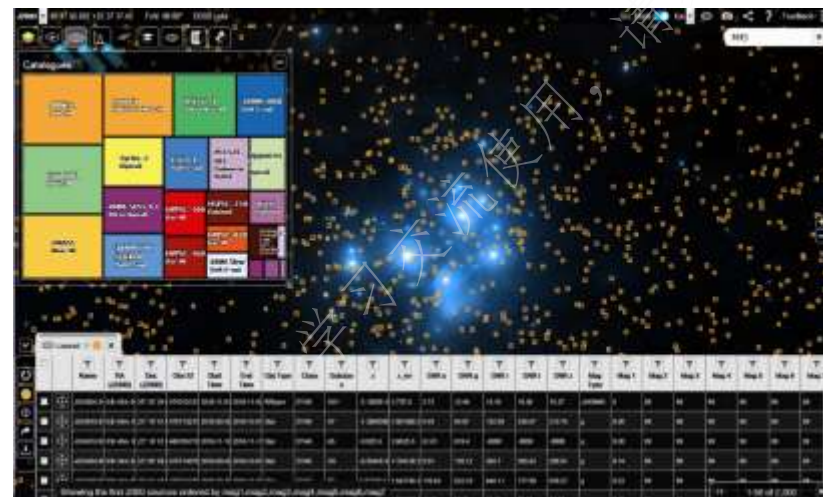
Collaborations with CDS & ESA

- **LAMOST datasets collected by ViziR/CDS from 2016**



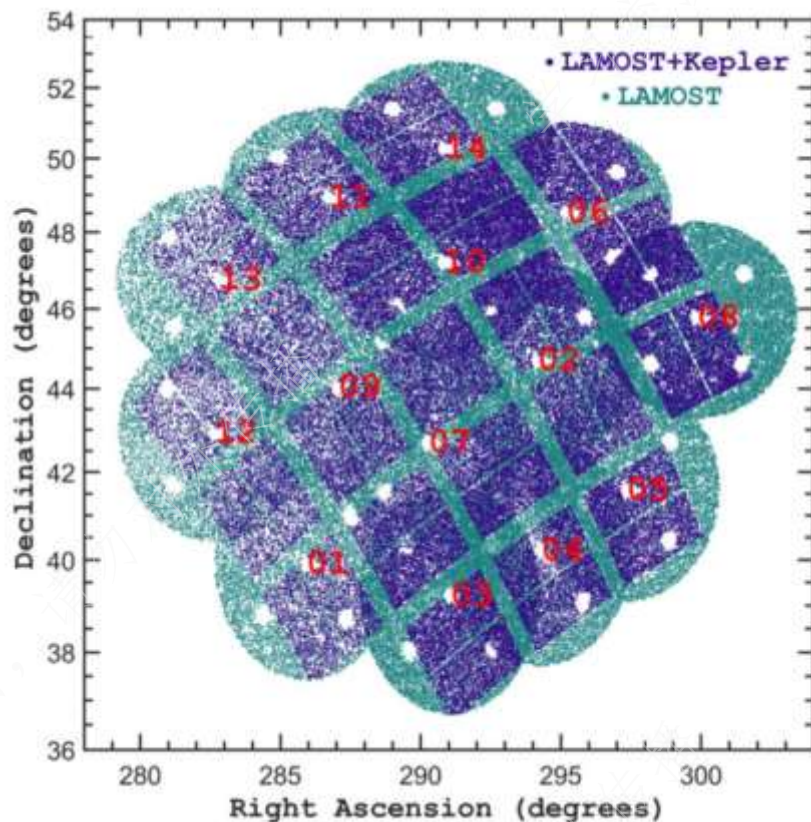
LAMOST DR5 in VizieR

- **Fusion with ESA Sky astronomical data system**



Collaboration with Kepler project

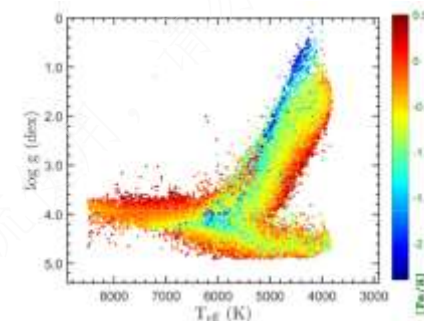
LAMOST-Kepler project (2012-2017, 2018...)



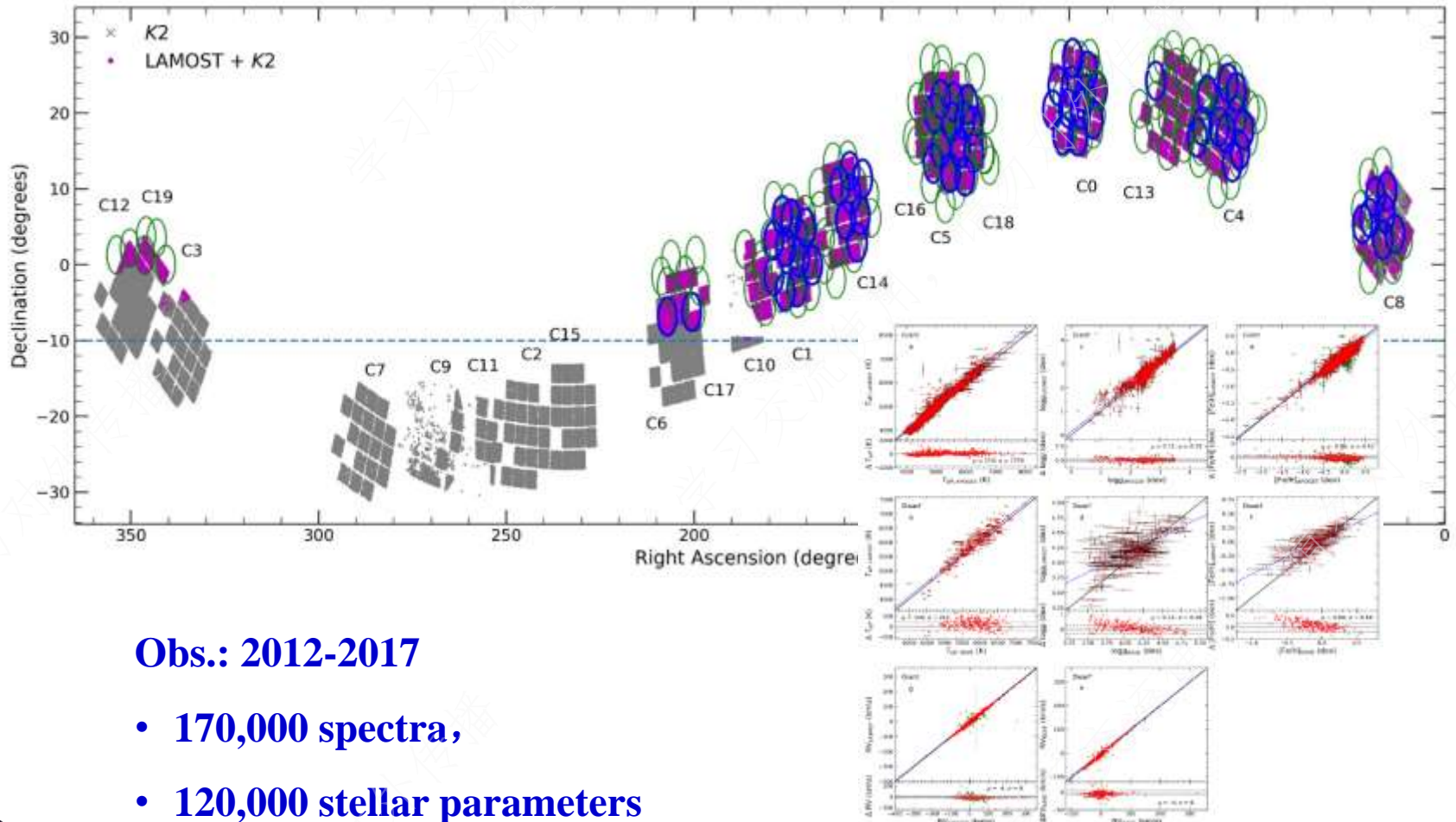
| Year | #Fields | #Plates | #Spectra |
|--------------|-----------|-----------|----------------|
| 2012 | 3 | 7 | 17,659 |
| 2013 | 6 | 14 | 39,309 |
| 2014 | 7 | 14 | 38,516 |
| 2015 | 11 | 32 | 97,247 |
| 2017 | 6 | 16 | 35,139 |
| 2018 | 1 | 2 | 4892 |
| <i>total</i> | <i>33</i> | <i>83</i> | <i>238,386</i> |

~39% of Kepler stars observed

De Cat & Fu et al. 2015, *ApJS*, 220, 19
Zong, Fu & De Cat et al. 2018, *ApJS*, 238, 30
Fu, De Cat & Zong, 2020, *RAA*, 20, 167



LAMOST-K2 project



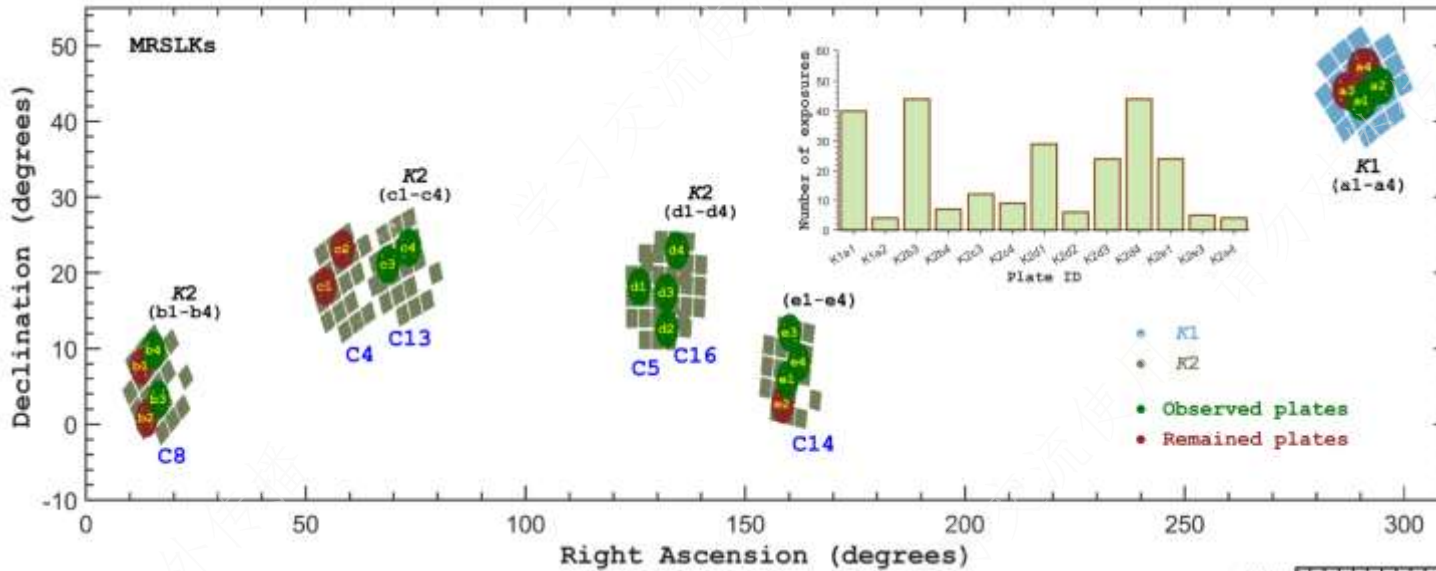
Obs.: 2012-2017

- 170,000 spectra,
- 120,000 stellar parameters
- K2 objects: 86,000 (~20%)

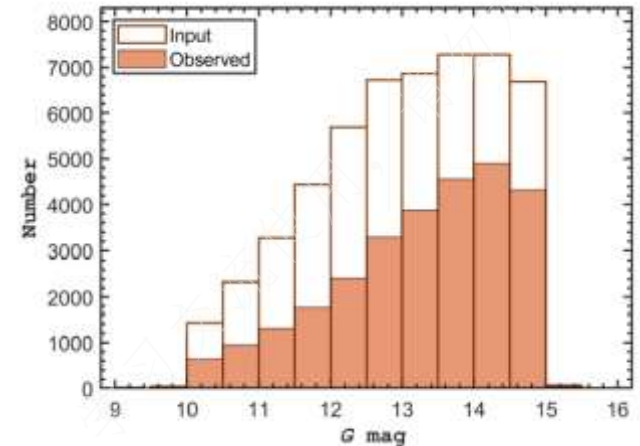
Wang, Fu & Zong et al. 2020, *ApJS*, 251, 27



Medium resolution survey for LAMOST-KEPLER/K2



- 20 plates in Kepler & K2 regions
- 50,000 stars
- 60 obs. for each plate

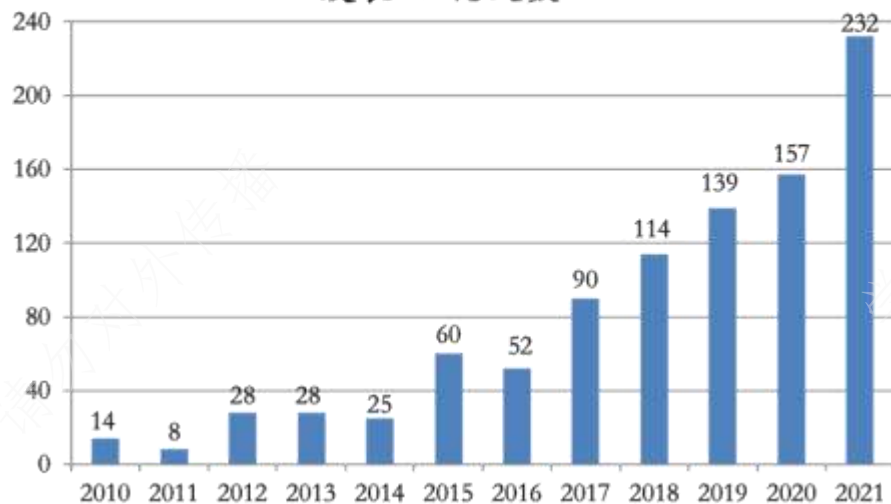


Publications by used of LAMOST data

No. of papers: 947

No. of citations:
10,394

2010-2021年利用LAMOST数据
发表SCI论文数



2010-2021年利用LAMOST数据
发表SCI论文的引文数



No. of papers by foreign astronomers

2010-2021年国外天文学家发表论文情况



| | 2017 | 2018 | 2019 | 2020 | 2021 |
|-----------------------------------|-------|-------|-------|-------|--------------|
| No. of SCI by foreign astronomers | 35 | 37 | 50 | 60 | 112 |
| No. of SCI by Chinese astronomers | 55 | 77 | 89 | 97 | 120 |
| Ratio | 38.9% | 32.5% | 36.0% | 39.3% | 48.3% |



Abundances in the Milky Way across Five Nucleosynthetic Channels from 4 Million LAMOST Stars

Show affiliations

Wheeler, Adam; Ness, Melissa; Buder, Sven; Bland-Hawthorn, Joss;
De Silva, Gayandhi; Hayden, Michael; Kos, Janez; Lewis, Geraint F.; Martell, Sarah;
Sharma, Sanjib; Simpson, Jeffrey D.; Zucker, D. B.; Zwitter, Tomaž

美国哥伦比亚大学
和澳大利亚悉尼大
学研究团队

Large stellar surveys are revealing the chemodynamical structure of the Galaxy across a vast spatial extent. However, the many millions of low-resolution spectra observed to date are yet to be fully exploited. We employ The Cannon, a data-driven approach for estimating chemical abundances, to obtain detailed abundances from low-resolution ($R = 1800$) LAMOST spectra, using the GALAH survey as our reference. We deliver five (for dwarfs) or six (for giants) estimated abundances representing five different nucleosynthetic channels, for 3.9 million stars, to a precision of 0.05-0.23 dex. Using wide binary pairs, we demonstrate that our abundance estimates provide chemical discriminating power beyond metallicity alone. We show the coverage of our catalog with radial, azimuthal and dynamical abundance maps and examine the neutron capture abundances across the disk and halo, which indicate different origins for the in situ and accreted halo populations. **LAMOST has near-complete Gaia coverage and provides an unprecedented perspective on chemistry across the Milky Way.**

LAMOST 基本覆盖
Gaia天区，对银河
系化学性质的研究
提供了前所未有的
视角

Publication: The Astrophysical Journal, Volume 898, Issue 1, id.58

Pub Date: July 2020

DOI: [10.3847/1538-4357/ab9a46](https://doi.org/10.3847/1538-4357/ab9a46) 

(Wheeler et al. 2020, ApJ, 898)

A stellar stream remnant of a globular cluster below the metallicity floor

<https://doi.org/10.1038/s41586-021-04162-2>

Received: 14 June 2021

Accepted: 19 October 2021

Published online: 5 January 2022

 Check for updates

Nicolas F. Martin^{1,2,3}, Kim A. Venn², David S. Aguado^{4,5,6}, Else Starckenburg⁷, Jonay I. González Hernández^{2,8}, Rodrigo A. Ibata¹, Piercarlo Bonifacio⁹, Elisabetta Caffau⁹, Federico Sestito³, Anke Arentsen¹, Carlos Allende Prieto^{5,8}, Raymond G. Carlberg¹⁰, Sébastien Fabbro^{3,11}, Morgan Fouesneau⁷, Vanessa Hill¹², Pascale Jablonka^{3,13}, Georges Kordopatis¹², Carmela Lardo¹⁴, Khyati Malhan¹⁵, Lyudmila I. Mashonkina¹⁶, Alan W. McConnachie¹⁷, Julio F. Navarro², Rubén Sánchez-Janssen¹⁷, Guillaume F. Thomas^{5,8}, Zhen Yuan¹ & Alessio Mucciarelli^{14,18}

Stellar ejecta gradually enrich the gas out of which subsequent stars form, making the least chemically enriched stellar systems direct fossils of structures formed in the early Universe¹. Although a few hundred stars with metal content below 1,000th of the solar iron content are known in the Galaxy^{2–4}, none of them inhabit globular clusters, some of the oldest known stellar structures. These show metal content of at least approximately 0.2% of the solar metallicity ($[Fe/H] \geq -2.7$). This metallicity floor appears universal^{5,6}, and it has been proposed that protogalaxies that merged into the galaxies we observe today were simply not massive enough to form clusters that survived to the present day⁷. Here we report observations of a stellar stream, C-19, whose metallicity is less than 0.05% of the solar metallicity ($[Fe/H] = -3.38 \pm 0.06$ (statistical) ± 0.20 (systematic)). The low metallicity dispersion and the chemical abundance stream is the tidal remnant of the most metal-poor globular cluster that is significantly below the purported metallicity floor and is significantly below the purported metallicity floor than observed today existed in the past Milky Way halo.

Research group from France, Canada, Italy, China et al.

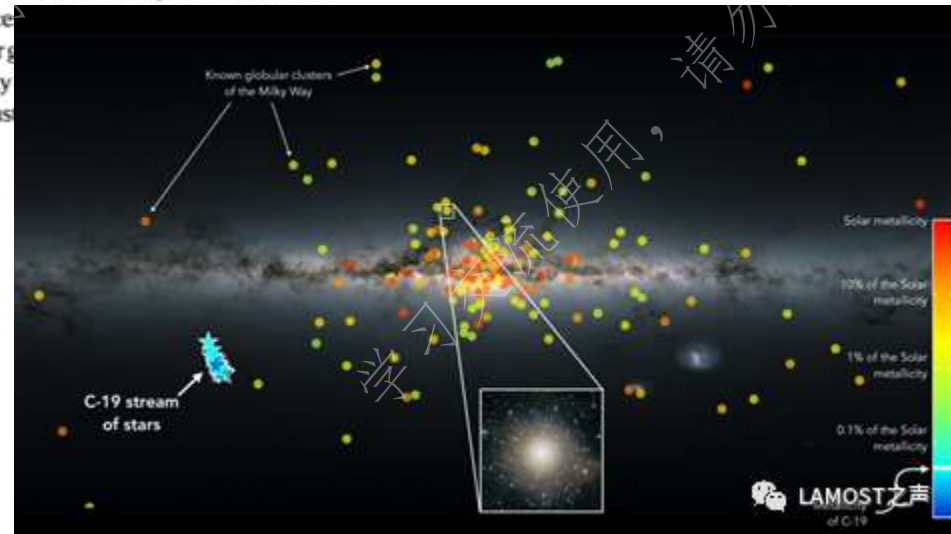
Z. Yuan: LAMOST fellow

C-19: stellar stream

LAMOST: 1 star

Gemini N: 3 stars

GTC: 6 stars

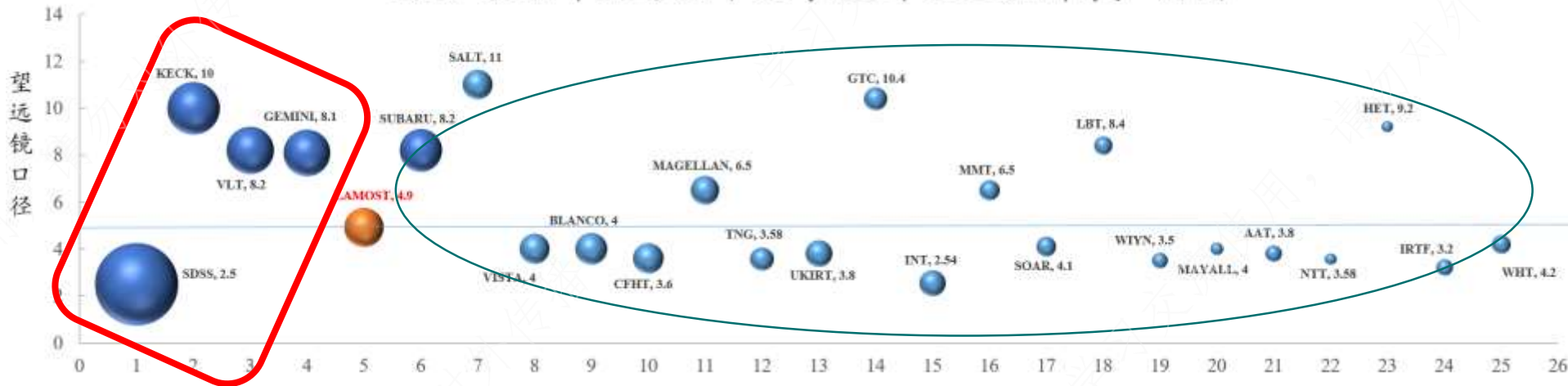


Publications by optical telescopes

Jan. 2017 – Dec. 2021

LAMOST is the 5th with the 25 O/IR telescopes in the world

2017-2021年全球25个光学/红外望远镜科学产出图

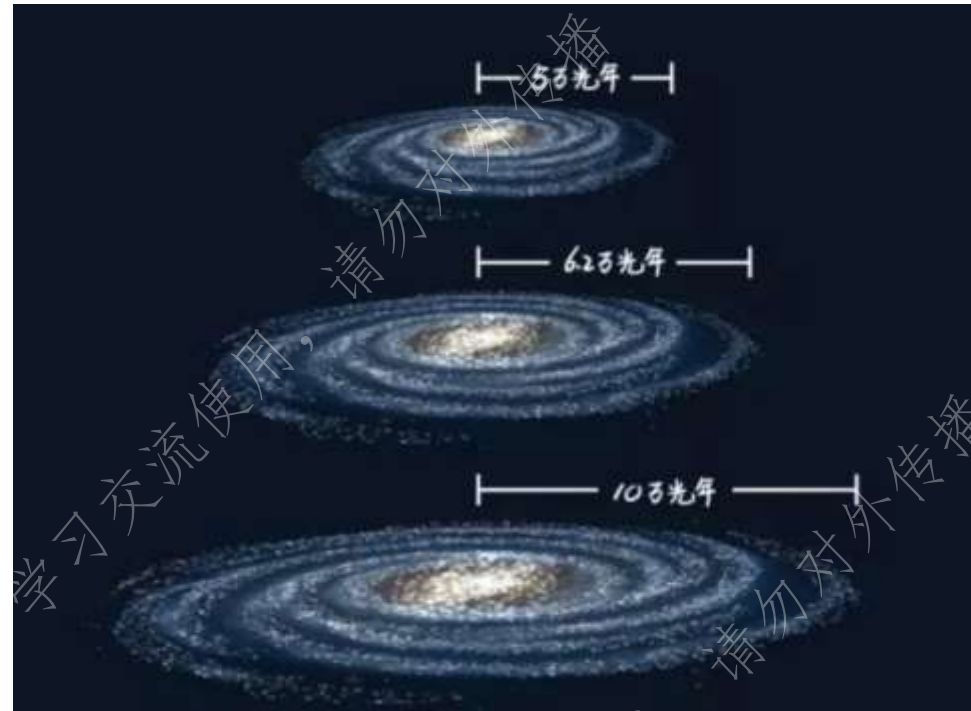


LAMOST sciences



Structure of the galactic disk: radius

- In textbook
50,000 light years
- 2017:
Liu et al. RAA
62,000 light years
- 2018:
Lopez-Corredoira et al. AA
100,000 light years
- 2021:
Li et al. ApJ
97,800 light years

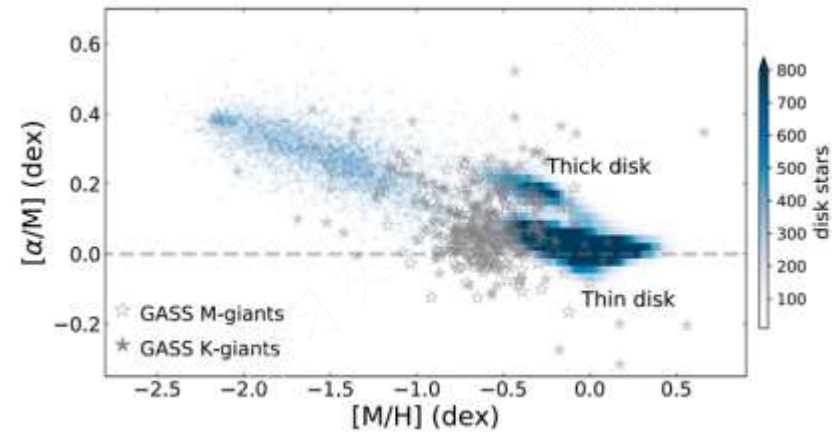
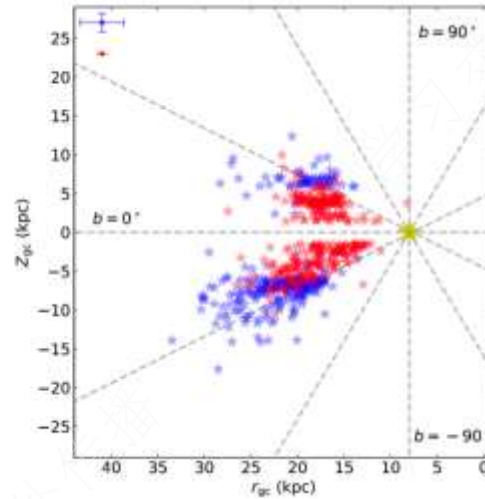
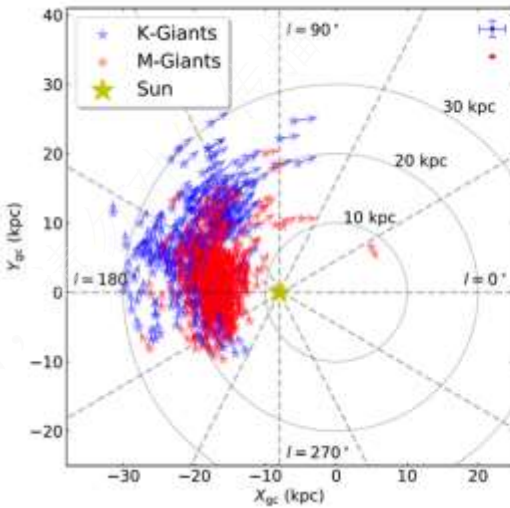
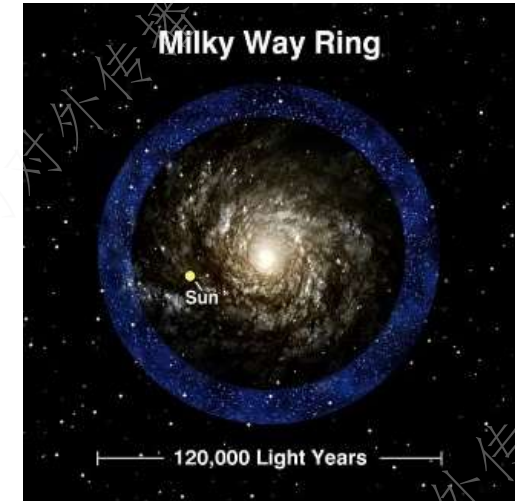


银盘半径大小变化示意图

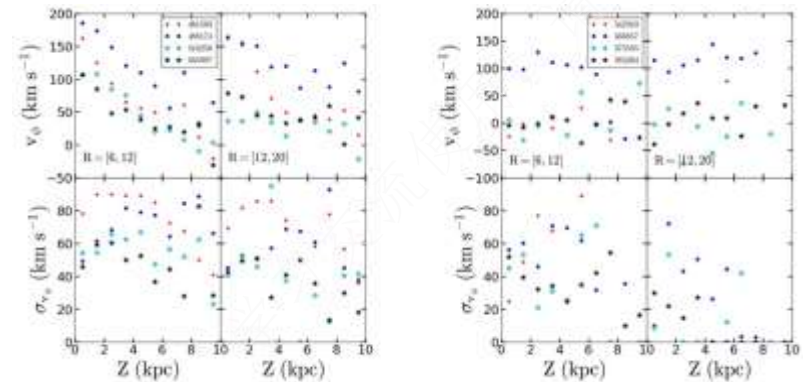
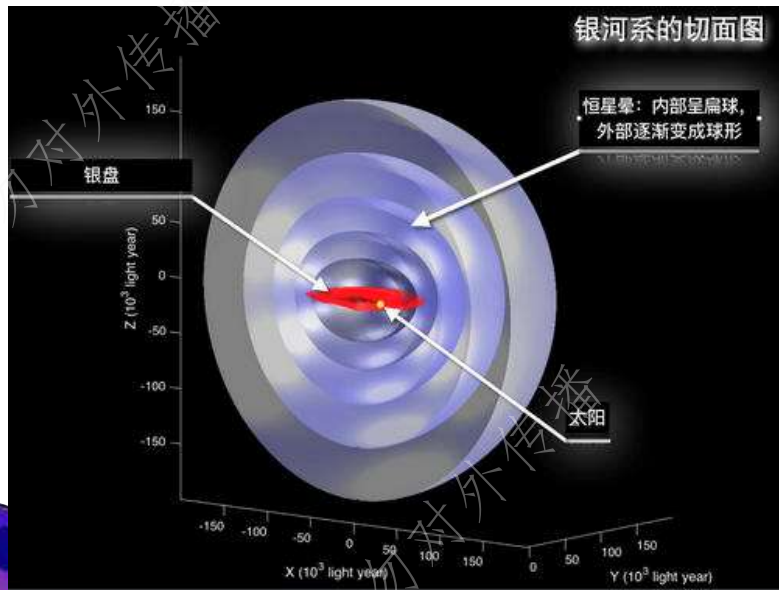
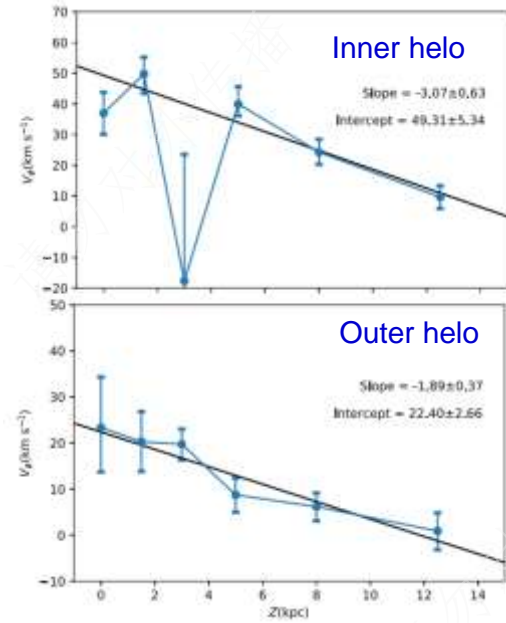
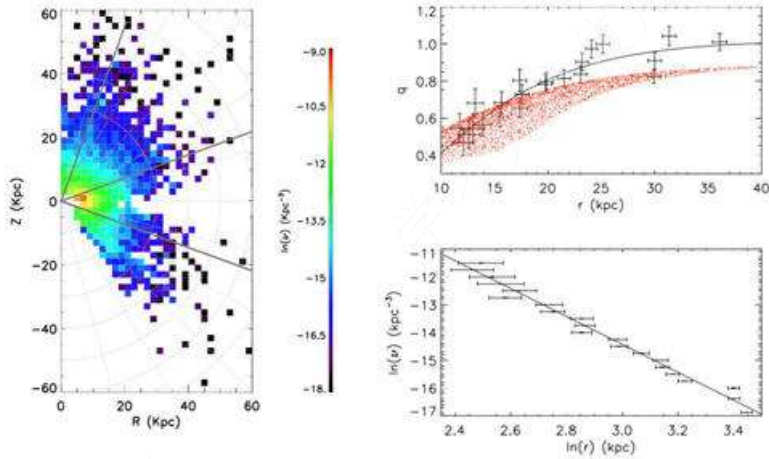


Monoceros ring

- Origin from disk
- Extended to 30 kpc

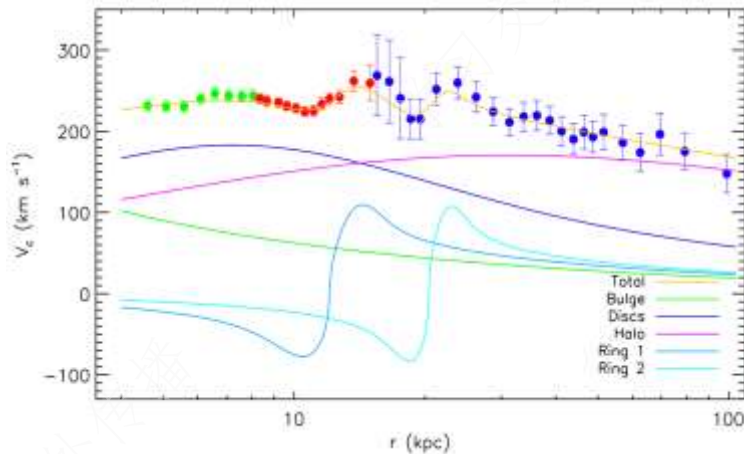


Structure of the halo



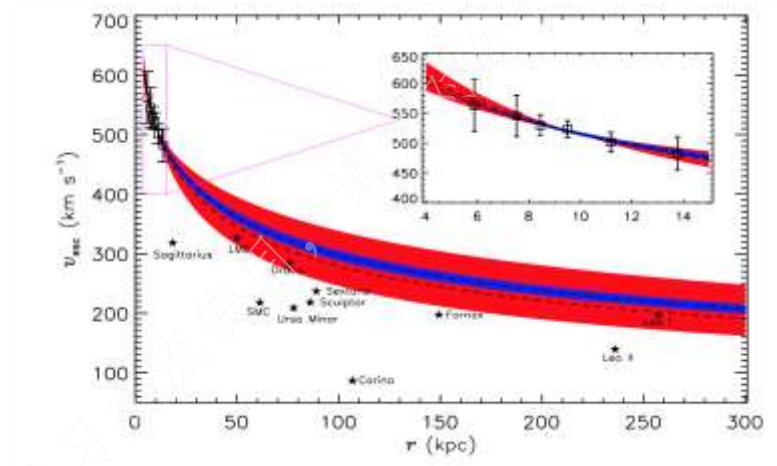
Total Mass of the Milky Way

$$M_{\text{Vir}} = 0.90 (+0.07, -0.08) \times 10^{12} M_{\odot}$$
$$\rho_{\text{DM}} = 0.32 (+0.02, -0.02) \text{ GeV cm}^{-3}$$



Huang et al. 2016

$$M_{\text{vir}} = (0.91 \pm 0.05) \times 10^{12} M_{\odot}$$
$$v_{\text{esc}}(R_0) = 529 \pm 29 \text{ km/s}$$



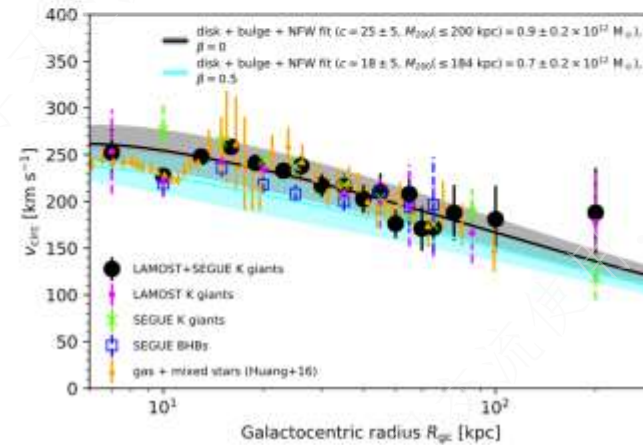
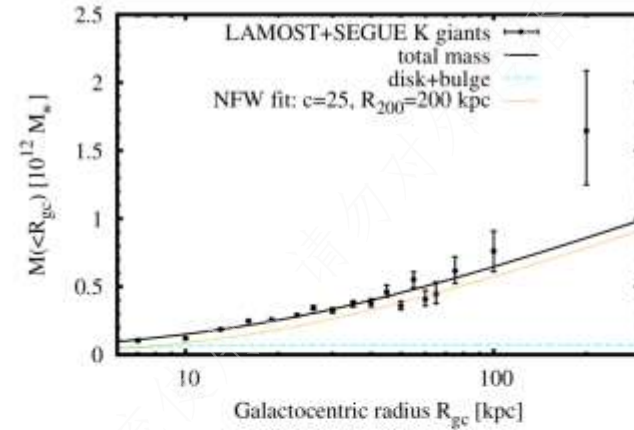
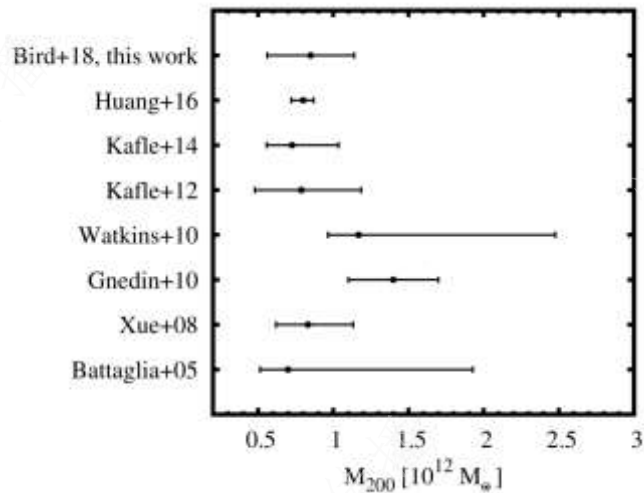
Huang et al. submitted

- Hitherto the most accurate Galactic **rotation curve** extending to 100 kpc based on 12000 selected from LSS-GAC DR2 and 4000 selected from APOGEE low Galactic latitude ($|b| < 3\sigma$) primary red clump stars, and 6000 halo K giants selected from SDSS
- Measurements of the Galactic **escape velocities** at Galactocentric radii between 5 and 14 are presented based on a sample of 527 high velocity halo stars ($|v_r| > 300 \text{ km/s}$, $[\text{Fe}/\text{H}] < -1$) selected from the LAMOST Galactic spectroscopic surveys



Star counts:

$$M_{200} = 0.85 \pm 0.05 \times 10^{12} \text{ Msun}$$



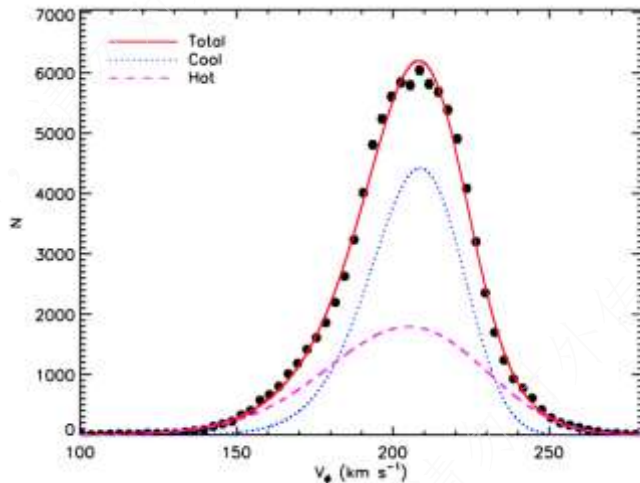
The Local Standard of Rest

Table 1. Measurements of the LSR in the literatures and from the current work.

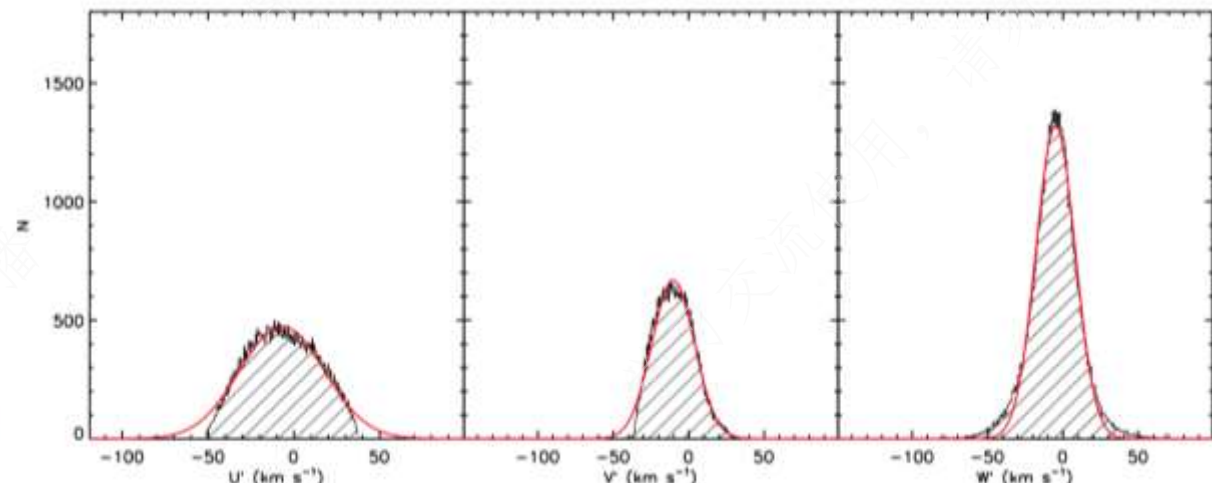
| Source | Data | U_{\odot} (km s^{-1}) | V_{\odot} (km s^{-1}) | W_{\odot} (km s^{-1}) |
|---------------------------|---------------------------------|---------------------------------------|---------------------------------------|---------------------------------------|
| This study (2014) | LSS-GAC DR1 | 7.01 ± 0.20 | 10.13 ± 0.12 | 4.95 ± 0.09 |
| Bobylev & Bajkova (2014) | Young objects | 6.00 ± 0.50 | 10.60 ± 0.80 | 6.50 ± 0.30 |
| Coşkunoğlu et al. (2011) | RAVE DR3 | 8.50 ± 0.29 | 13.38 ± 0.43 | 6.49 ± 0.26 |
| Bobylev & Bajkova (2010) | Masers | 5.50 ± 2.2 | 11.00 ± 1.70 | 8.50 ± 1.20 |
| Breddels et al. (2010) | RAVE DR2 | 12.00 ± 0.60 | 20.40 ± 0.50 | 7.80 ± 0.30 |
| Schönrich et al. (2010) | <i>Hipparcos</i> | $11.10^{+0.09}_{-0.75}$ | $12.24^{+0.47}_{-0.47}$ | $7.25^{+0.37}_{-0.36}$ |
| Reid et al. (2009) | Masers | 9.0 | 20 | 10 |
| Francis & Anderson (2009) | <i>Hipparcos</i> | 7.50 ± 1.00 | 13.50 ± 0.30 | 6.80 ± 0.10 |
| Bobylev & Bajkova (2007) | F & G dwarfs | 8.70 ± 0.50 | 6.20 ± 2.22 | 7.20 ± 0.80 |
| Piskunov et al. (2006) | Open clusters | 9.44 ± 1.14 | 11.90 ± 0.72 | 7.20 ± 0.42 |
| Mignard (2000) | K0-K5 | 9.88 | 14.19 | 7.76 |
| Dehnen & Binney (1998) | <i>Hipparcos</i> | 10.00 ± 0.36 | 5.25 ± 0.62 | 7.17 ± 0.38 |
| Binney et al. (1997) | Stars near South Celestial Pole | 11.00 ± 0.60 | 5.30 ± 1.70 | 7.00 ± 0.60 |
| Mihalas & Binney (1981) | Galactic Astronomy (2nd Ed.) | 9.00 | 12.00 | 7.0 |
| Homann (1886) | Solar neighbourhood stars | 17.40 ± 11.2 | 16.90 ± 10.90 | 3.60 ± 2.30 |

- Based on 94,332 thin disk FGK dwarfs within 600 pc of the Sun.
 $(U_{\odot}, V_{\odot}, W_{\odot}) = (7.01 \pm 0.20, 10.13 \pm 0.12, 4.95 \pm 0.09) \text{ km/s}$
- V is 2 times of one in “Galactic Dynamics” (Dehnen & Binney 1998)

Method I: VDF



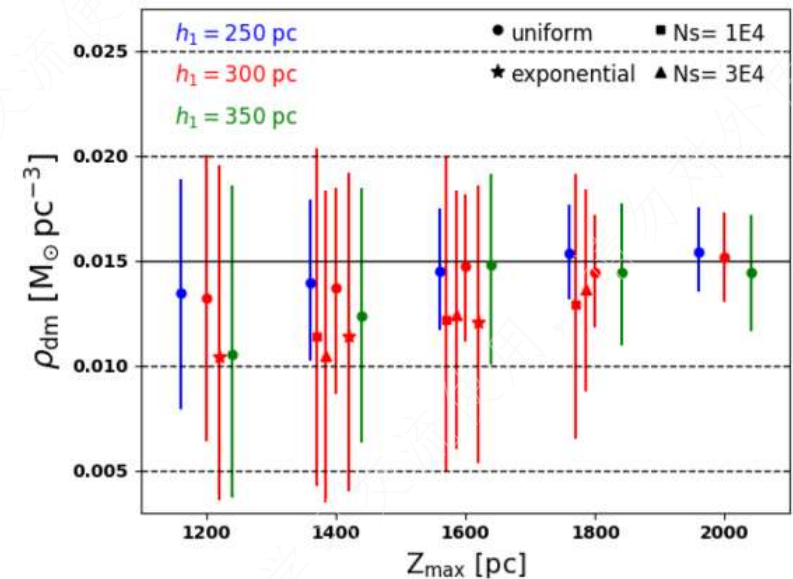
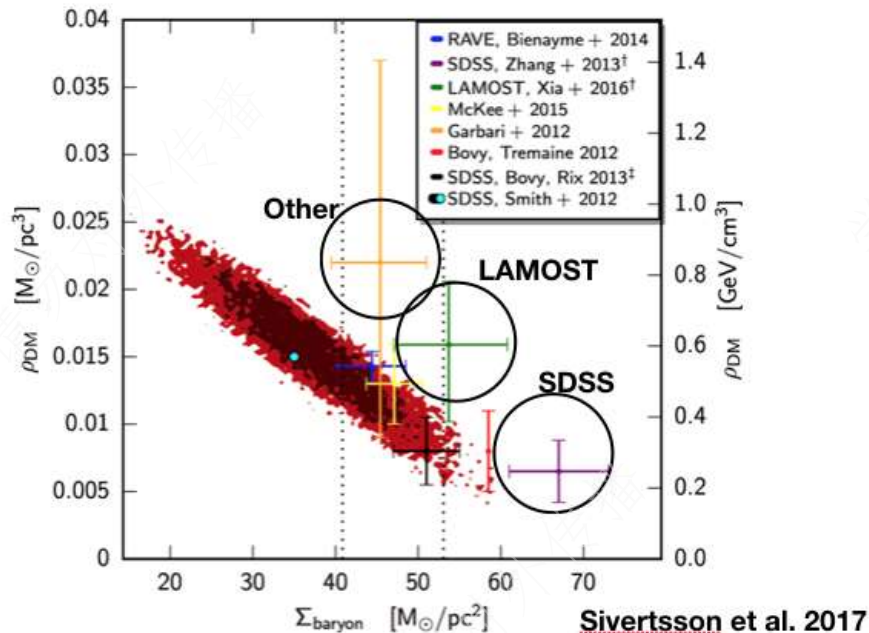
Method II: CTDS



Dark matter mass density in the solar neighborhood

- With LAMOST data and a simple analytical Kz force model depending on less assumptions
- the volume density of the dark matter around us is $0.018 \pm 0.005 M_{\odot} \text{pc}^{-3}$

We apply the vertical Jeans equation to the kinematics of Milky Way stars in the solar neighbourhood to measure the local dark matter density. More than 90 000 G- and K-type dwarf stars are selected from the cross-matched sample of LAMOST (Large Sky Area Multi-Object Fibre Spectroscopic Telescope) fifth data release and *Gaia* second data release for our analyses. The mass models applied consist of a single exponential stellar disc, a razor thin gas disc, and a constant dark matter density. We first consider the simplified vertical Jeans equation that ignores the tilt term and assumes a flat rotation curve. Under a Gaussian prior on the total stellar surface density, the local dark matter density inferred from Markov chain Monte Carlo simulations is $0.0133^{+0.0024}_{-0.0022} M_{\odot} \text{pc}^{-3}$. The local dark matter densities for subsamples in an azimuthal angle range of $-10^{\circ} < \phi < 5^{\circ}$ are consistent within their 1σ errors. However, the



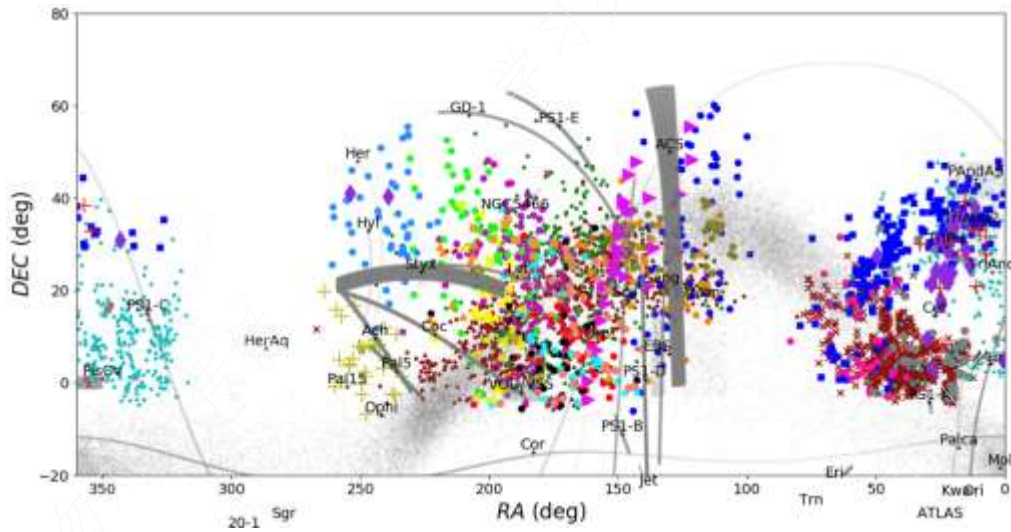
Xia, Liu, et al., MNRAS, 2016

Guo, Liu, et al., MNRAS, 2020



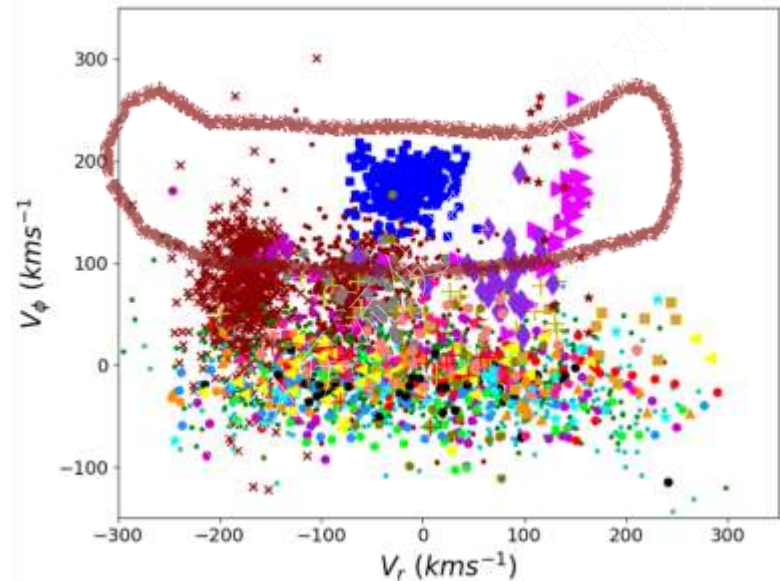
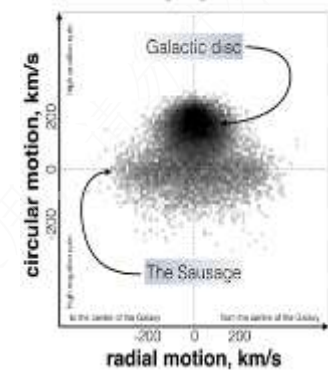
Stellar stream in the halo

LAMOST K giants



- Monoceros Ring
- Sagittarius streams
- Orphan stream
- Cetus stream
- Gaia-Sausage

Motions of 7,000,000 Gaia stars



Yang, Xue et al. ApJ, 2019a



Stellar stream in the halo

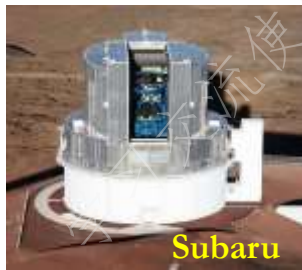
- 33000 M giants in DR4
- 3d space orbit of the Sgr stream
- The far side in 130 kpc from the Sun



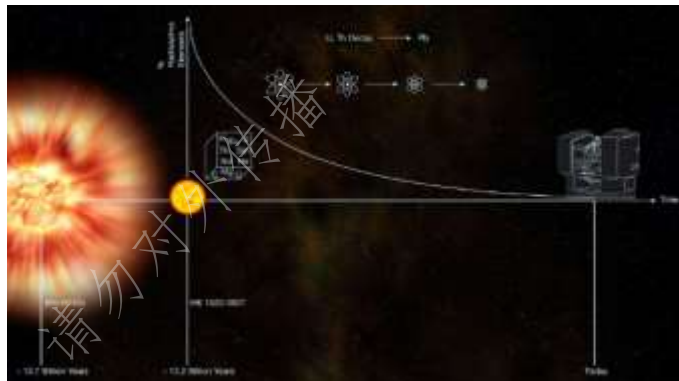
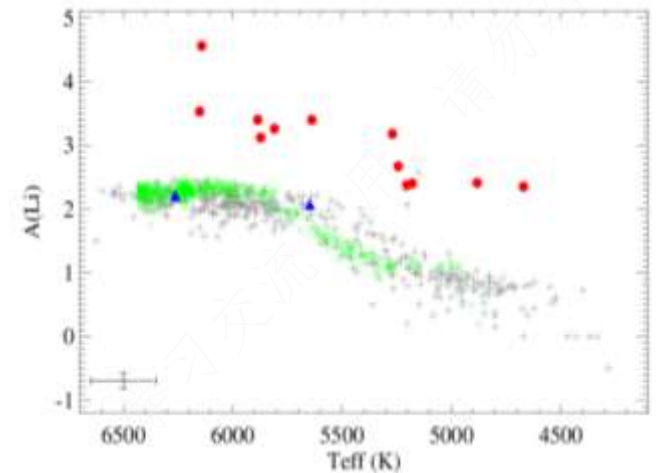
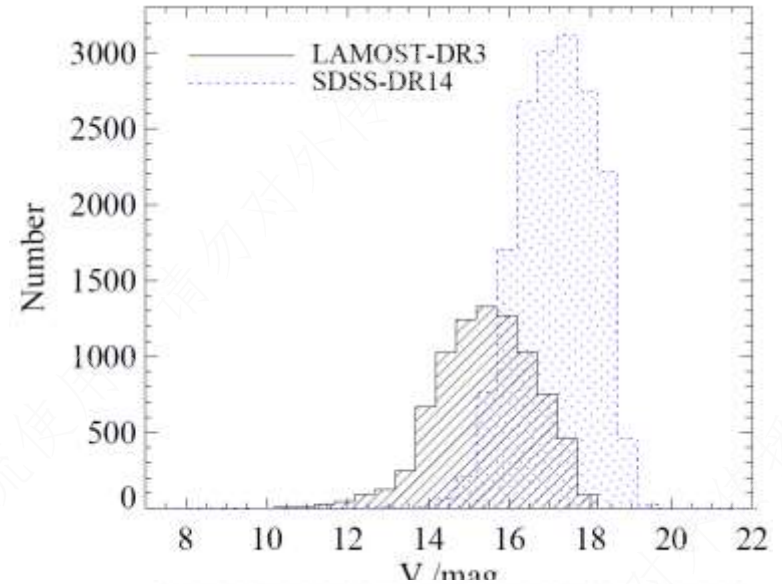
Li et al. 2019, ApJ, 874, 138



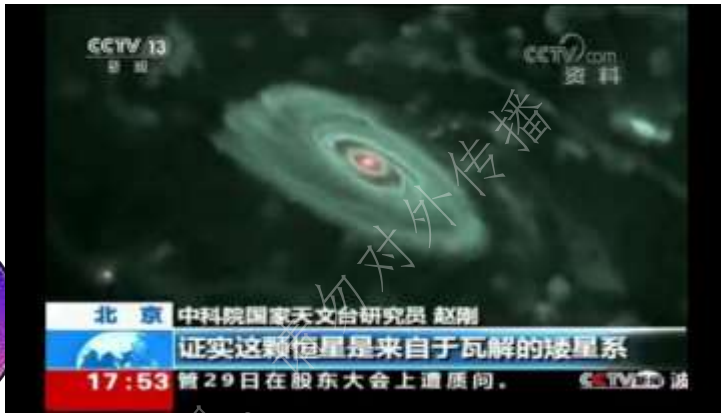
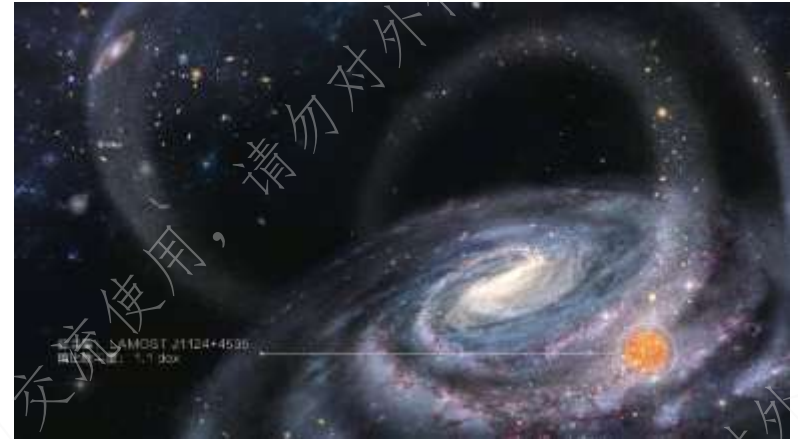
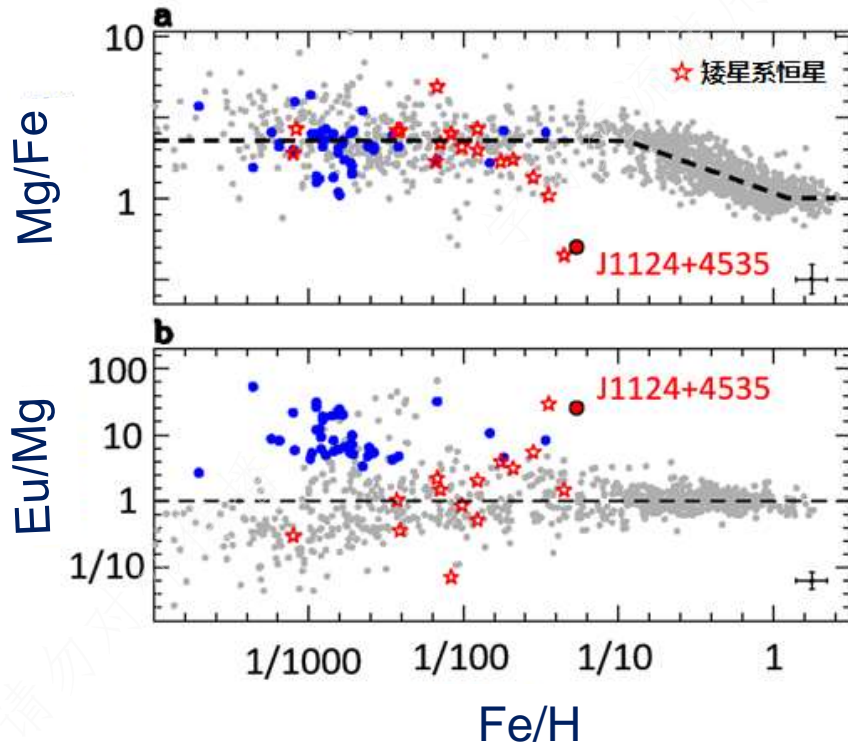
Metal-poor stars



- 100,000 candidates of bright metal-poor stars
- 90% to search $[Fe/H] < -2$
- “Millstone” sample:
400 high resolution spectra



Evidence for the accretion origin of a halo star



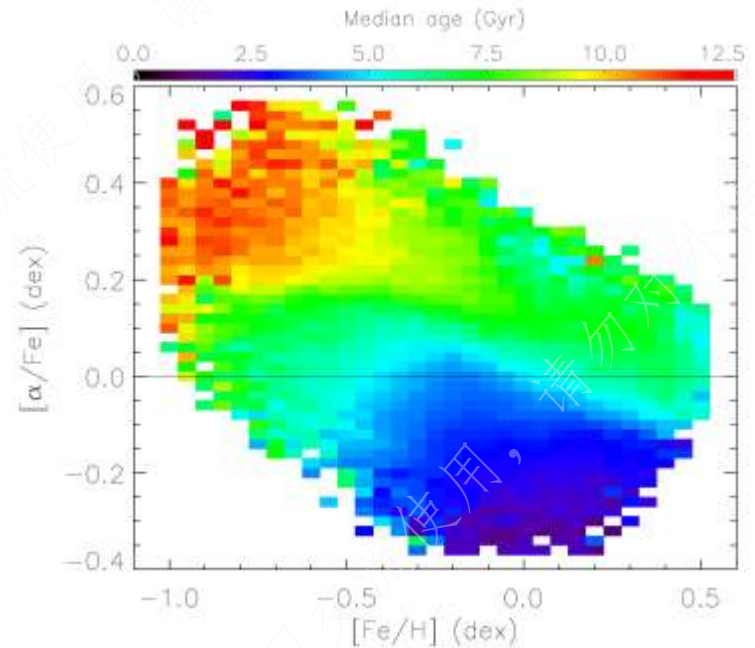
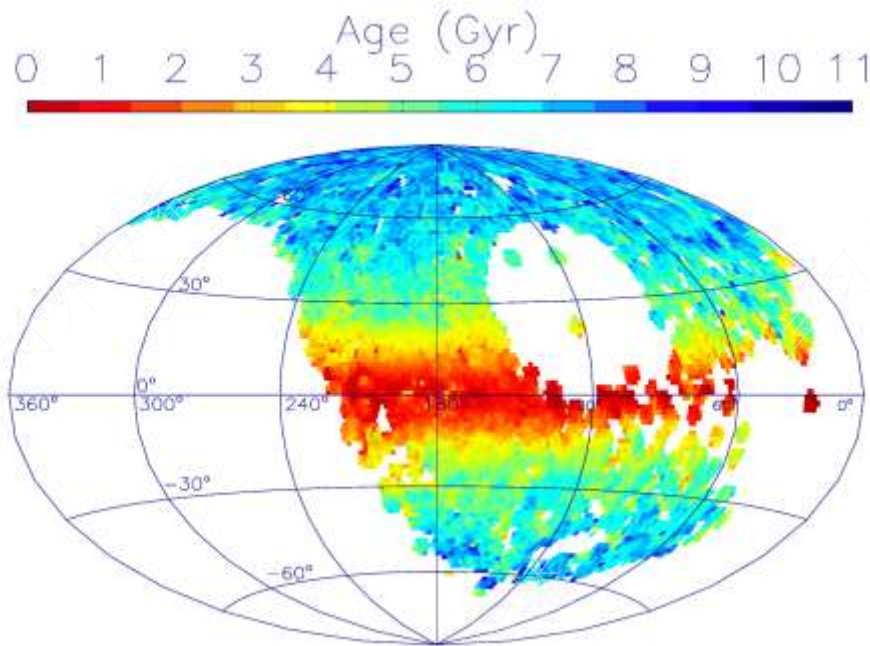
Evidence for the accretion origin of halo stars with an extreme r-process enhancement

Qian-Fan Xing^{1*}, Gang Zhao^{1*}, Wako Aoki^{2,3}, Satoshi Honda⁴, Hai-Ning Li¹, Miho N. Ishigaki¹ and Tadafumi Matsuno^{2,3}

Xing et al. 2019, *Nature Astronomy*, 3, 631

Ages of 1,000,000 stars

- Turn-off stars: 1 M (Xiang et al. 2015, 2017)
- RC stars: 0.2 M
- Red giants : 0.64 M



Reviewer's Comments: This is a solid body of work that makes a significant contribution to the field, and which is especially valuable as a benchmark for Galactic evolution modeling.



Article

A time-resolved picture of our Milky Way's early formation history

<https://doi.org/10.1038/s41586-022-04496-5>

Maosheng Xiang^{1,2*} & Hans-Walter Rix^{1,2*}

M. Xiang: LAMOST fellow

Received: 1 November 2021

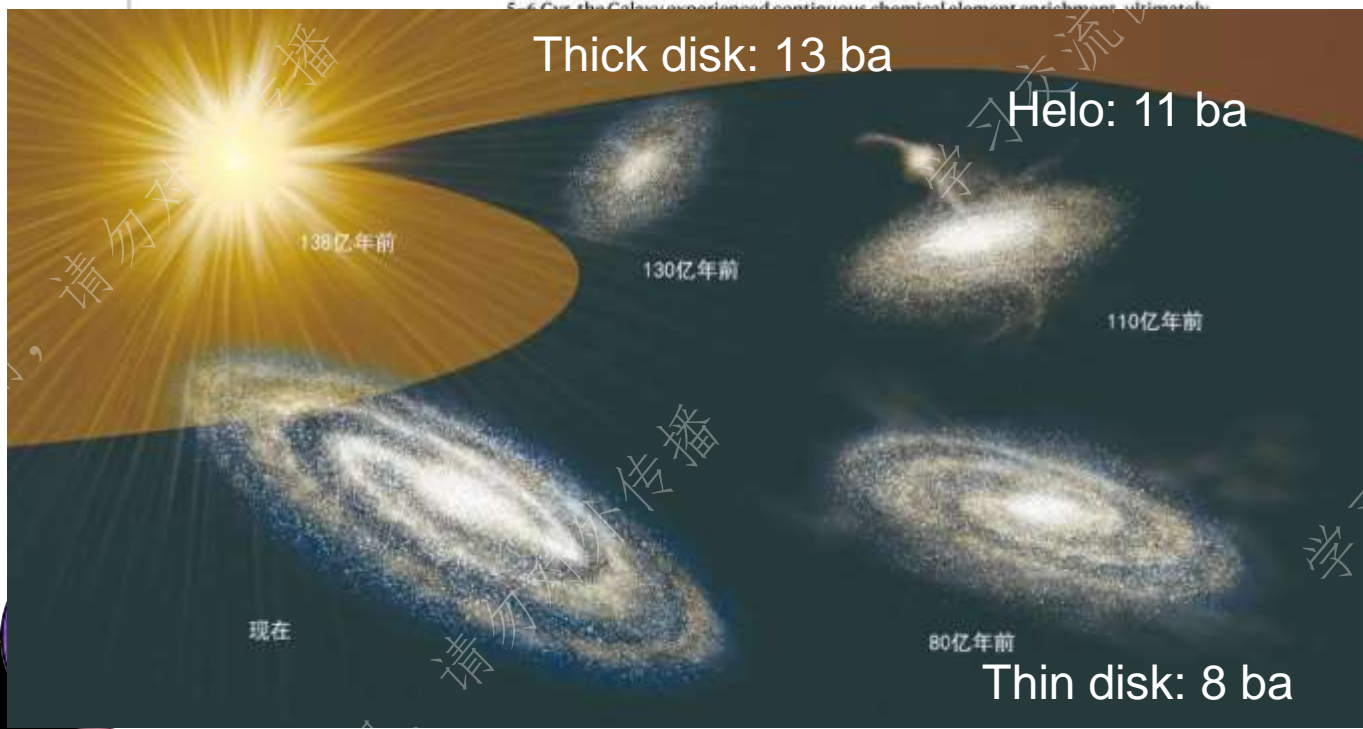
Accepted: 1 February 2022

Published online: 23 March 2022

Open access

Check for updates

The formation of our Milky Way can be split up qualitatively into different phases that resulted in its structurally different stellar populations: the halo and the disk components^{1–3}. Revealing a quantitative overall picture of our Galaxy's assembly requires a large sample of stars with very precise ages. Here we report an analysis of such a sample using subgiant stars. We find that the stellar age–metallicity distribution $p(r, [Fe/H])$ splits into two almost disjoint parts, separated at age $\tau \approx 8$ Gyr. The younger part reflects a late phase of dynamically quiescent Galactic disk formation with manifest evidence for stellar radial orbit migration^{4–6}; the other part reflects the earlier phase, when the stellar halo⁷ and the old α -process-enhanced (thick) disk^{8,9} formed. Our results indicate that the formation of the Galaxy's old (thick) disk started approximately 13 Gyr ago, only 0.8 Gyr after the Big Bang, and 2 Gyr earlier than the final assembly of the inner Galactic halo. Most of these stars formed around 11 Gyr ago, when the Gaia-Sausage-Enceladus satellite merged with our Galaxy^{10,11}. Over the next 5–6 Gyr, the Galaxy experienced continuous chemical element enrichment, ultimately



Thick disk: 13 ba

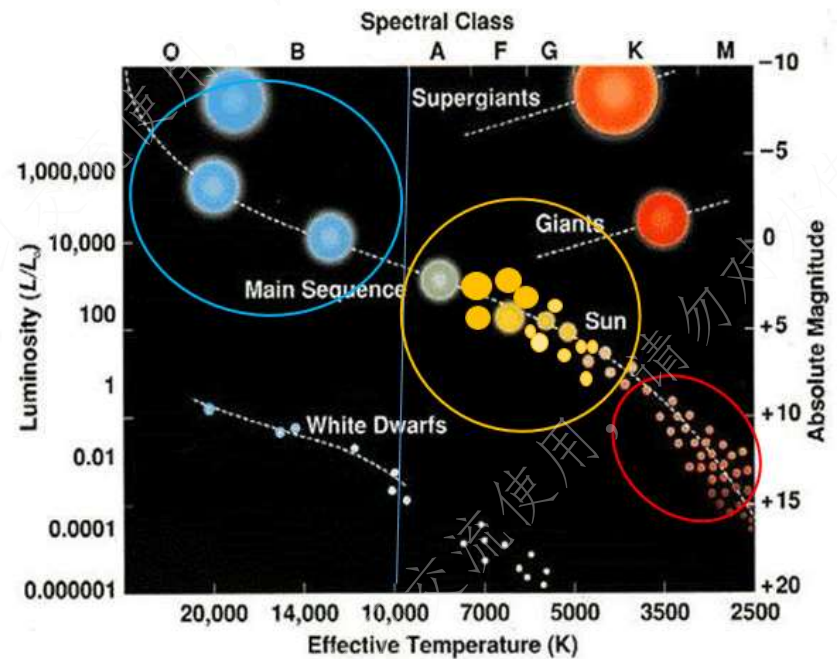
Halo: 11 ba

Thin disk: 8 ba

- LAMOST DR7
- Gaia eDR3
- 250,000 sub-giants
- age < 7%

The largest OB catalog

- OB stars: high temperature, high mass, short life, rare
- 16032 OB stars discovered by LAMOST
- The fundamental data for young stars in the out disk of the Galaxy



Liu et al. 2019, ApJS, 241, 32



New Oe stars

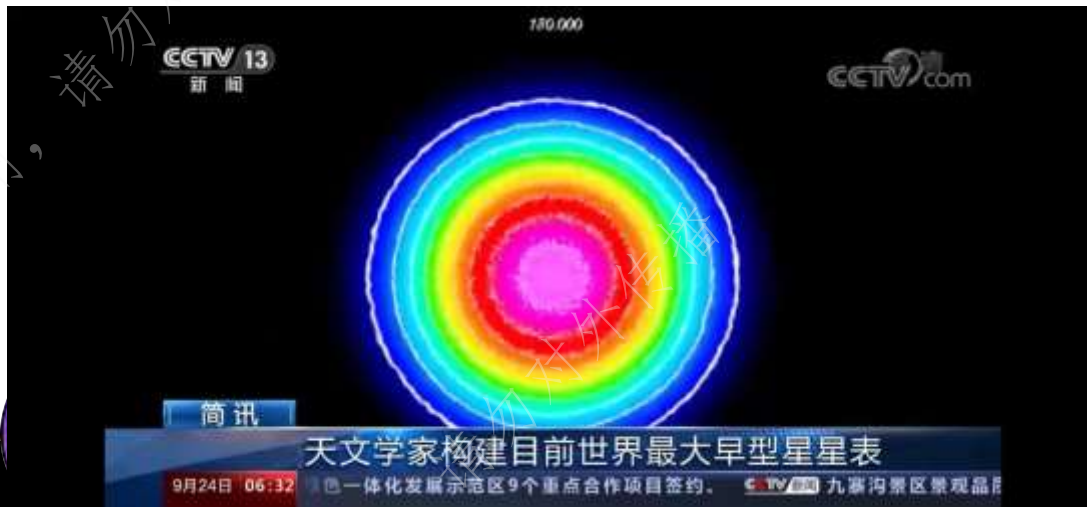
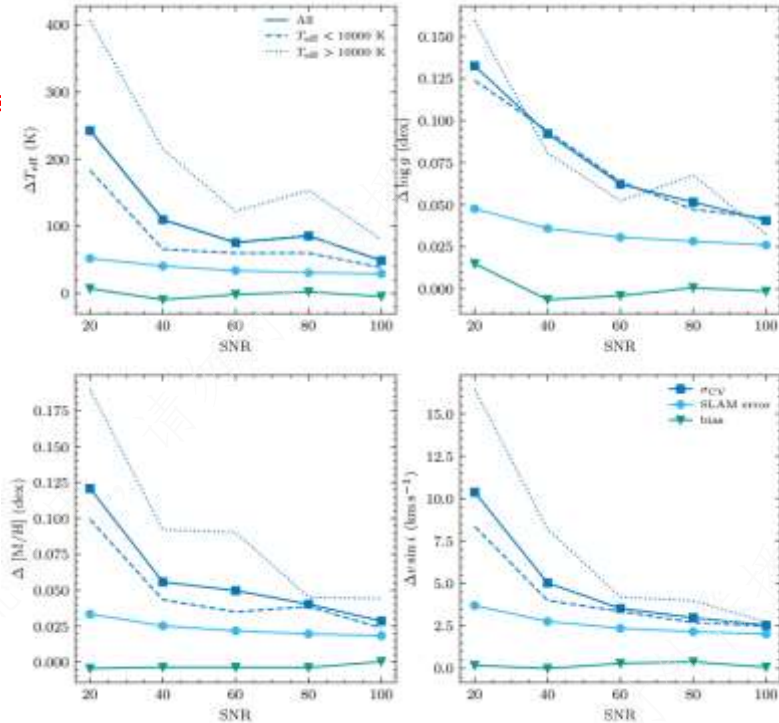
-
-
- **Oe star: very few**
 - high speed rotation
 - with disk
 - **6 Oe stars discovered by LAMOST, 13 Oe stars in total before**
 - **To understand the origin of the Oe stars**



Early-type stars

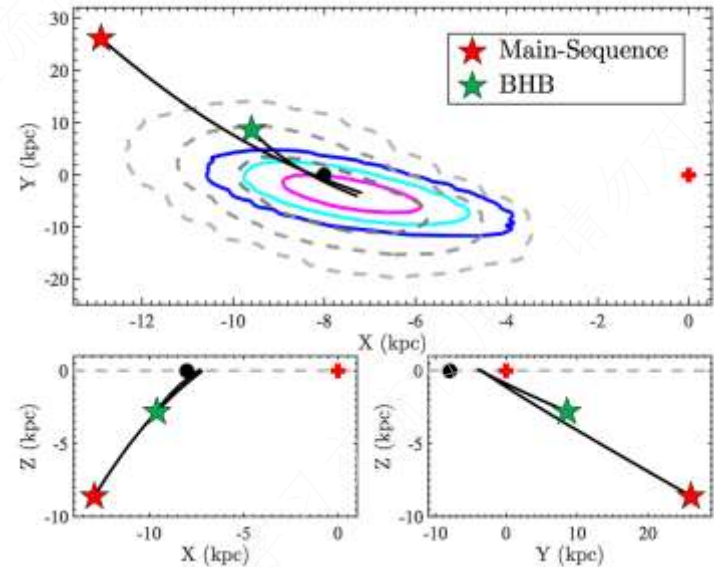
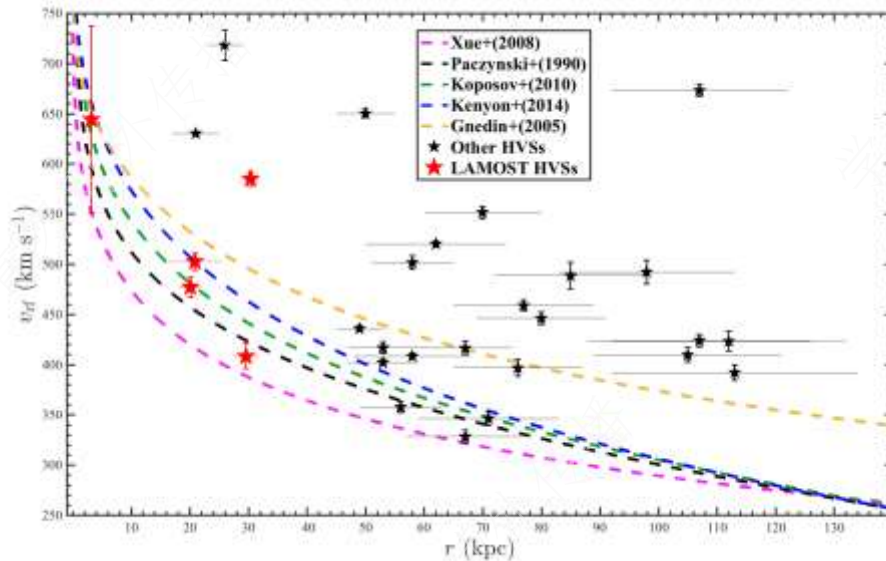
- 40,034 early-type stars with $v_{\text{sin}i}$, T_{eff} , $\log g$, $[M/H]$

Medium resolution observed by LAMOST



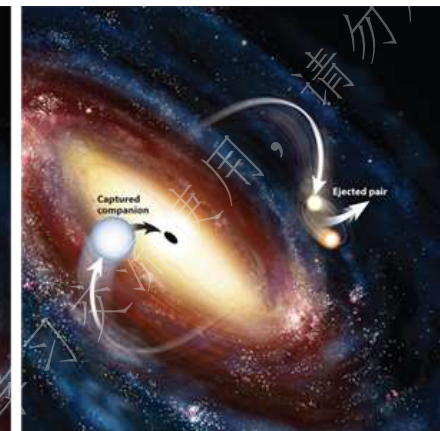
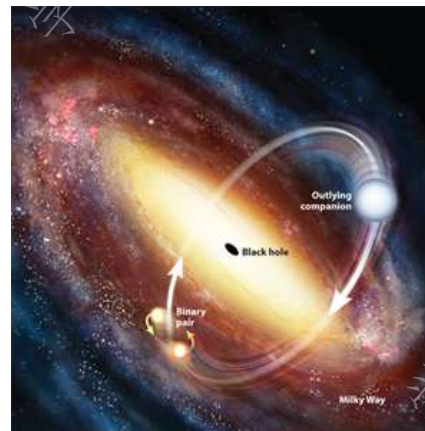
Hyper-velocity stars: 4 from LAMOST

- Letter of prof. Brown: “an exciting pair of hypervelocity star discoveries”
- Websites: Universe Today, Phys.org, AAS Nova



High-velocity stars

- 591 high-velocity stars (2x before)
- 42 candidates of hyper-velocity stars (2x before)



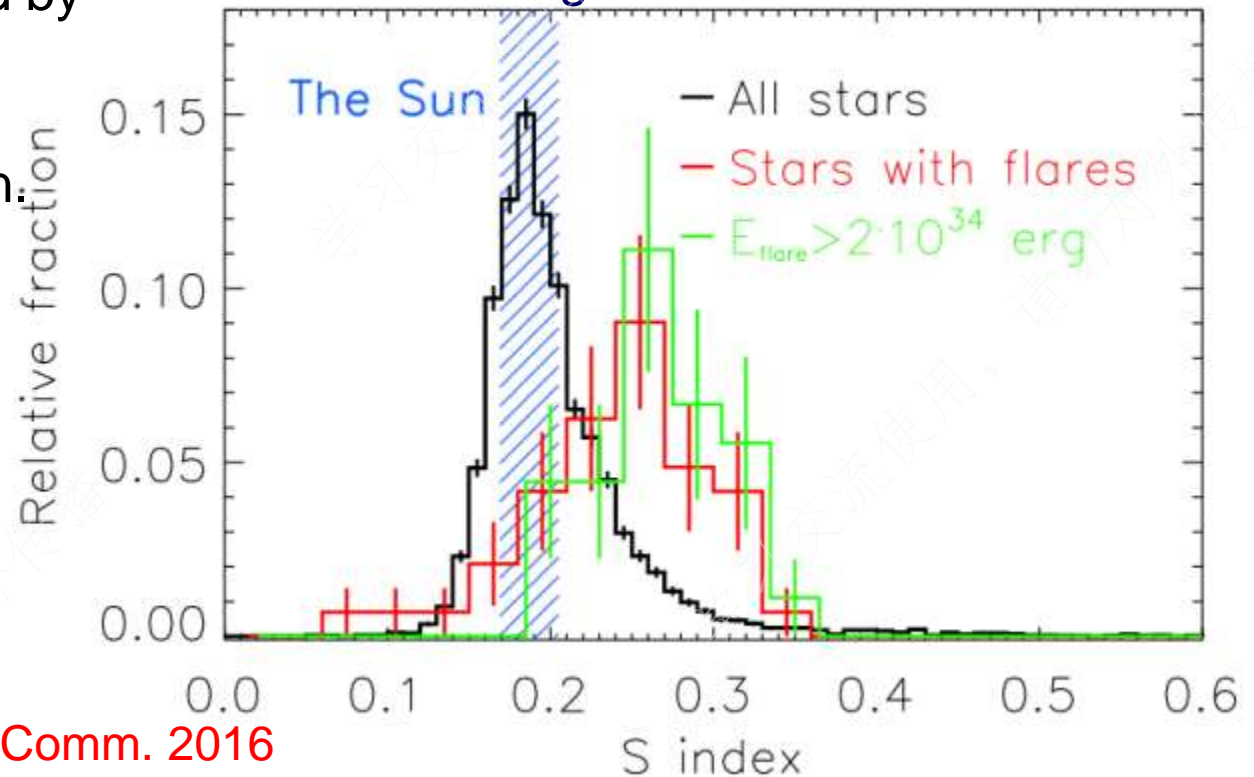
Superflare stars characterised by enhanced magnetic activity

- 5648 solar-like stars
- 48 superflare stars.

Superflare stars are generally characterised by larger chromospheric emissions than other stars, including the Sun.



1-6 orders higher than solar flares



Highest Li abundance in the Li-rich giants

Highest Li abundance
in the Li-rich giants



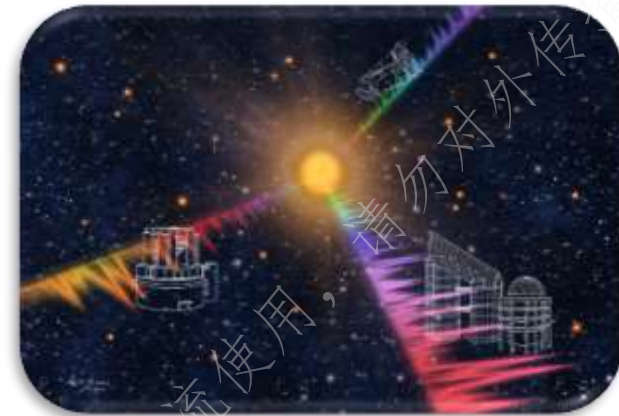
Yan et al. 2018, Nature Astronomy

Li produced by solar-like
stars



Kumar et al. 2020, Nature Astronomy

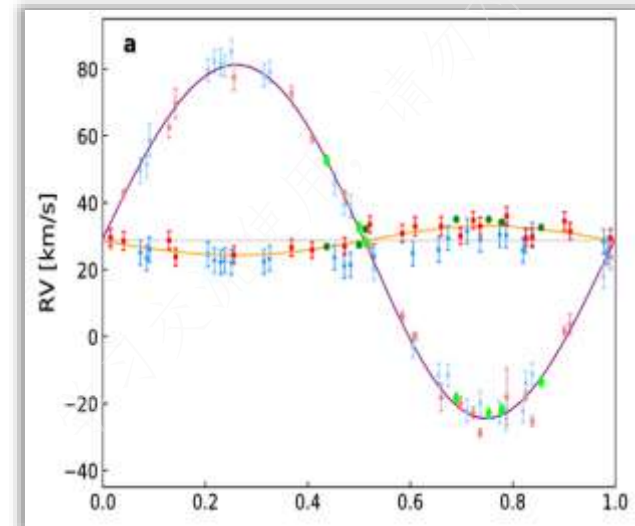
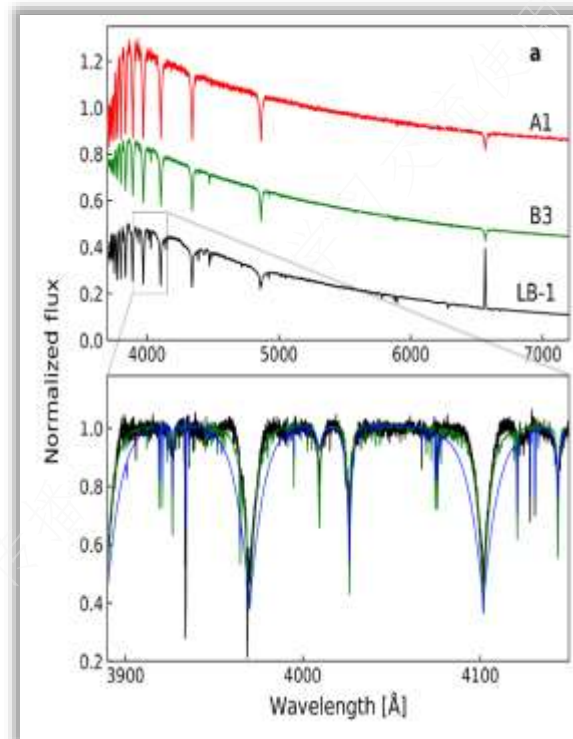
Li-rich in red clump
stars, not in red giants



Yan et al. 2021, Nature Astronomy

Discovery of stellar-mass black hole

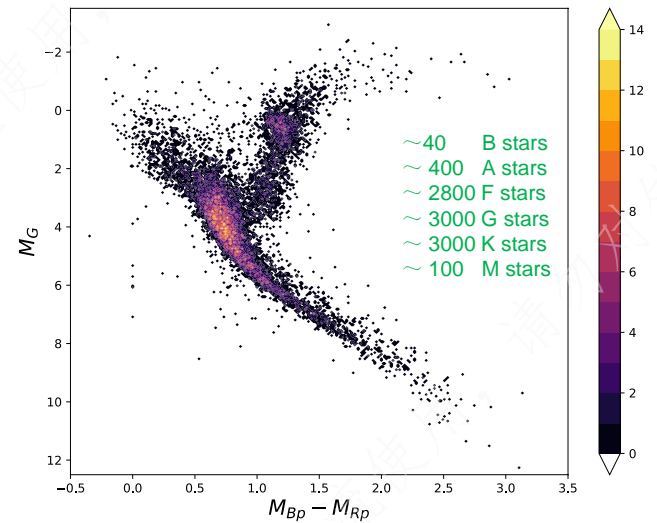
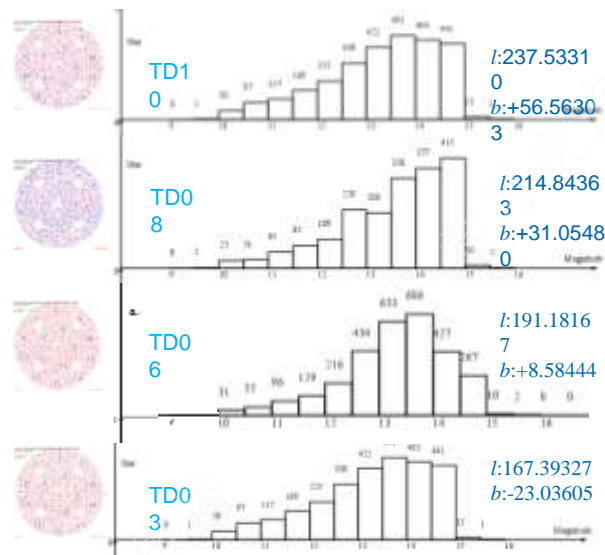
- **70 M_{\odot} black hole**
- **New method to discover black holes**



“Black-hole hunter”

黑洞猎手计划

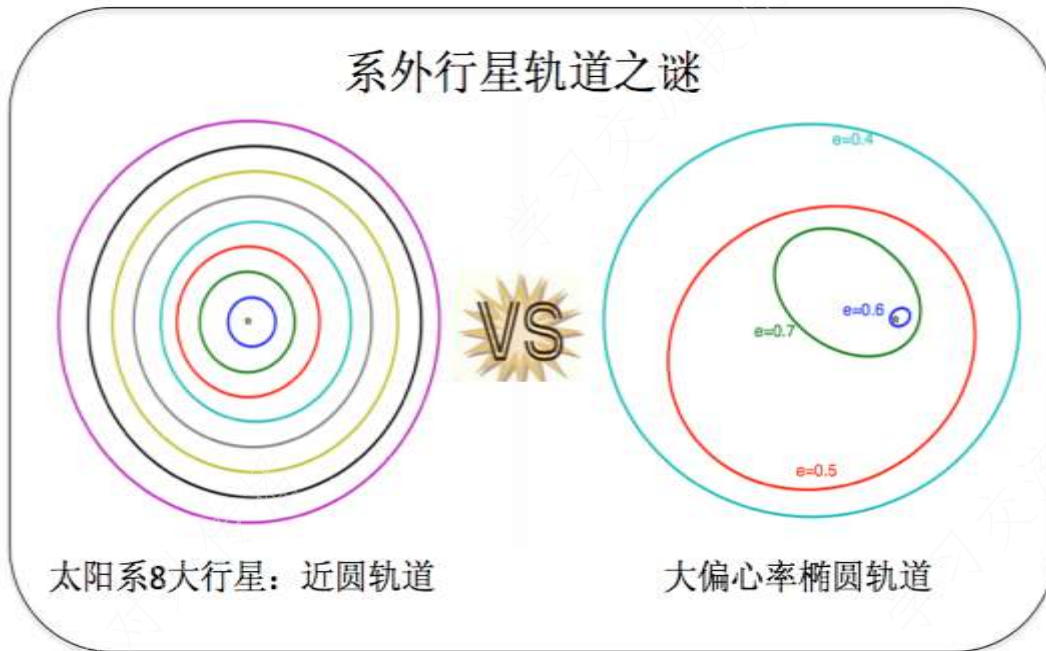
Four plates of LAMOST



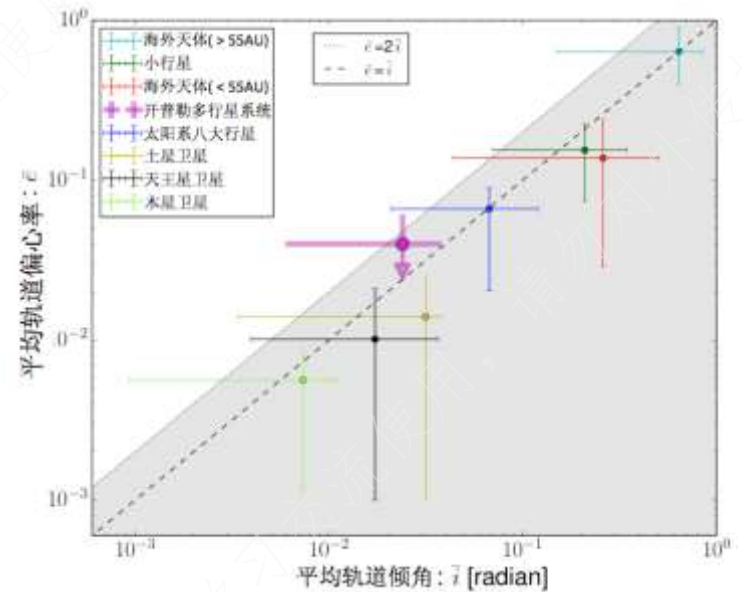
Wang et al. 2020b



Puzzle of Exoplanet Orbits



The eccentricity distributions for a large (698) and homogeneous Kepler planet sample with transit duration statistics.



The prevalence of circular orbits and the common relation may imply that the solar system as well as its formation is not so atypical in the Galaxy after all.

New type of exoplanets: Hoptunes

Proceedings of the National Academy of Sciences of the United States of America

www.pnas.org

From the Cover

- E226 Diversification of cicada endosymbionts
- 245 Proactive versus reactive aggression
- 266 Neptune-size cousins of hot Jupiters
- 349 DNA replication completion mechanism
- 421 Genetics, experience, and birdsong learning

January 9, 2018 | vol. 115 | no. 2

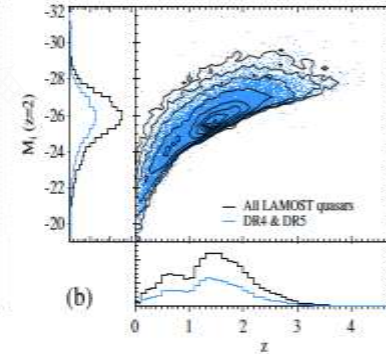
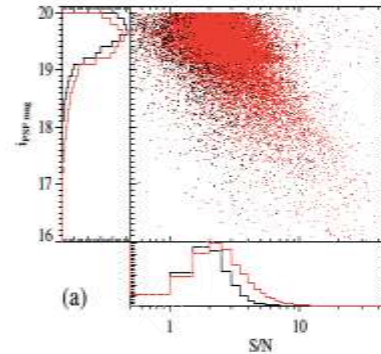


- 266 LAMOST telescope reveals that Neptunian cousins of hot Jupiters are mostly single offspring of stars that are rich in heavy elements
Subo Dong, Ji-Wei Xie, Ji-Lin Zhou, Zheng Zheng, and Ali Luo

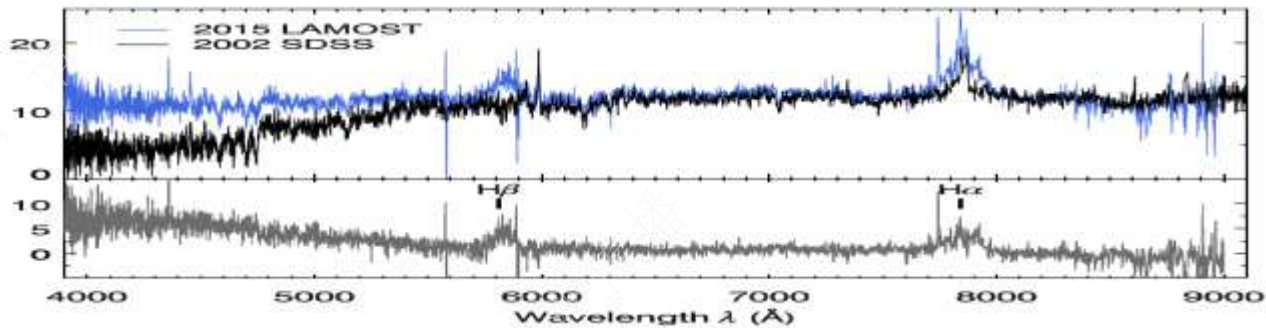
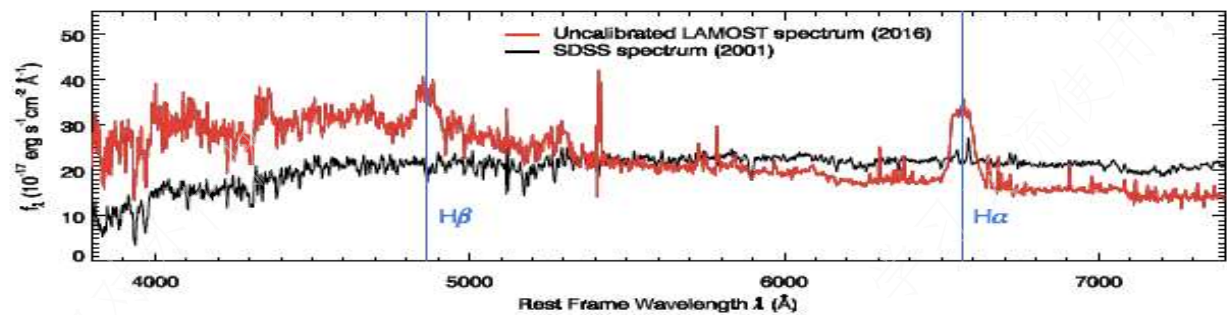
Dong & Xie et al., 2018, PNAS, 115, 266–271

LAMOST Quasar Survey

- Identified 56000 quasars
 - 28000 independently discovered
 - 22500 new discovered
 - **DR1:** Ai, Wu, Yang, et al., 2016, AJ, 151, 24
 - 3921 quasars identified, 1180 new
 - **DR2/DR3:** Dong, Wu, Ai, et al., 2018, AJ, 155, 189
 - 19935 identified, 12126 independent, 8100 new
 - **DR4/DR5:** Yao, Wu, Ai, et al., 2019, ApJS, 240, 6
 - 19246 identified, 11446 independent, 8149 new
 - **DR6-DR8:** Jin, Wu, Fu, et al., 2021, to be submitted
 - 12761 identified, 7071 independent, 5380 new
- LAMOST quasar survey has become one of the top 3 quasar surveys, after SDSS & 2dF.

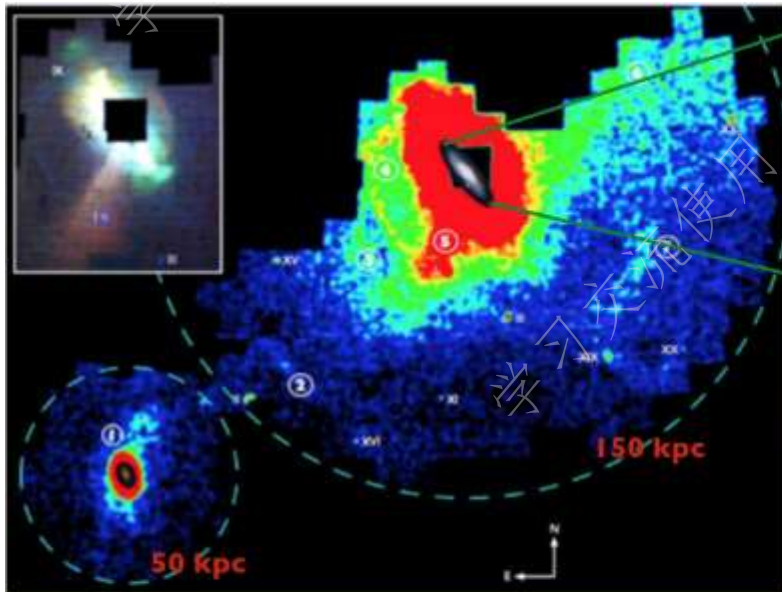


• 21 “face-change” QSOs



Yang et al. 2018

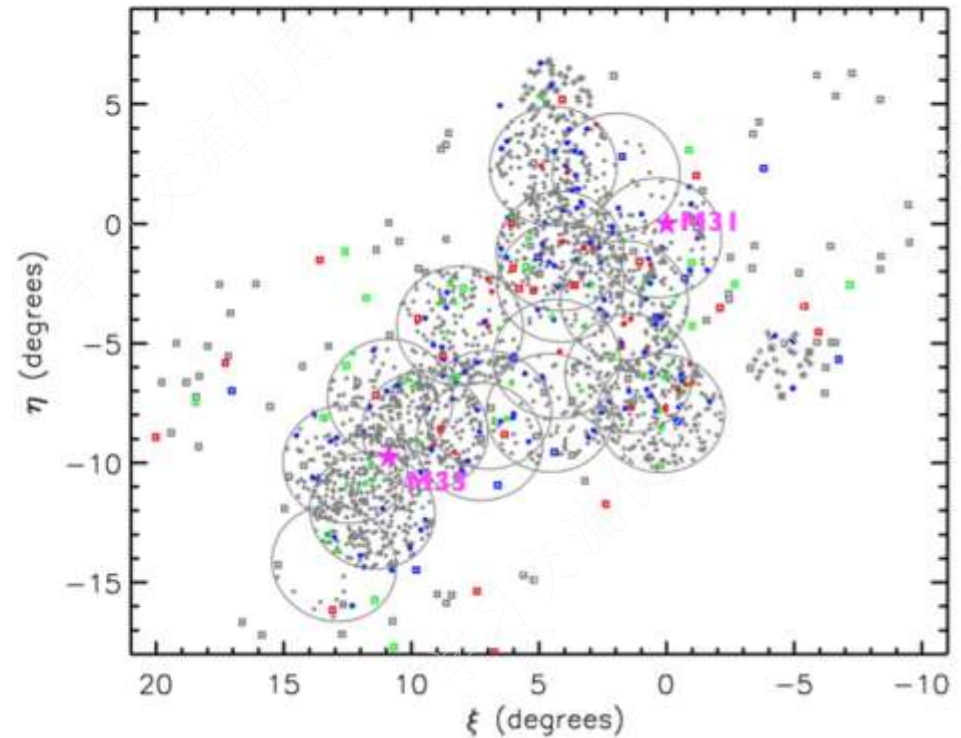




- 1, M33 structure;
 - 2, 125-kpc stream (stream A);
 - 3, stream C; 4, eastern arc (stream D);
 - 5, giant stellar stream;
 - 6, northwest minor-axis stream;
 - 7, southwest cloud
- (McConnachie et al. 2009)

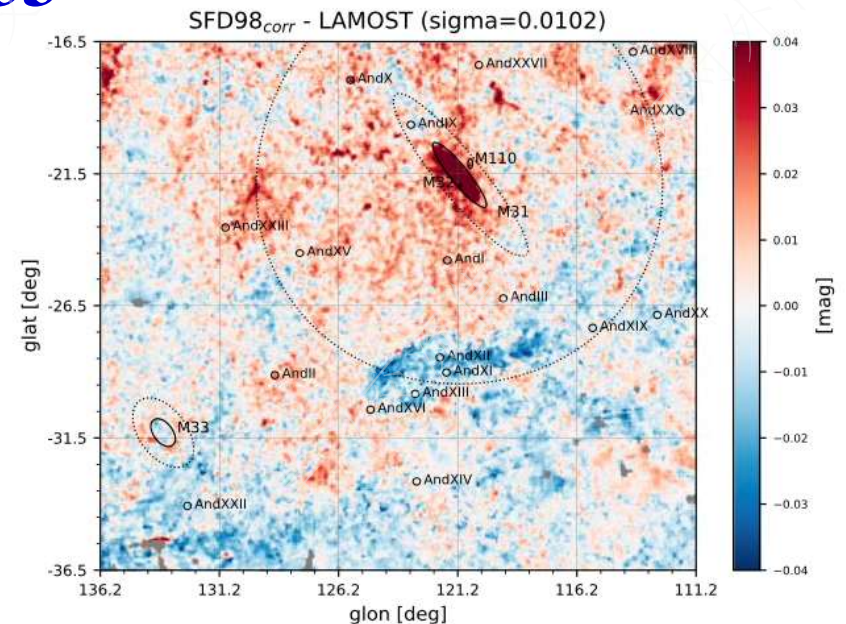
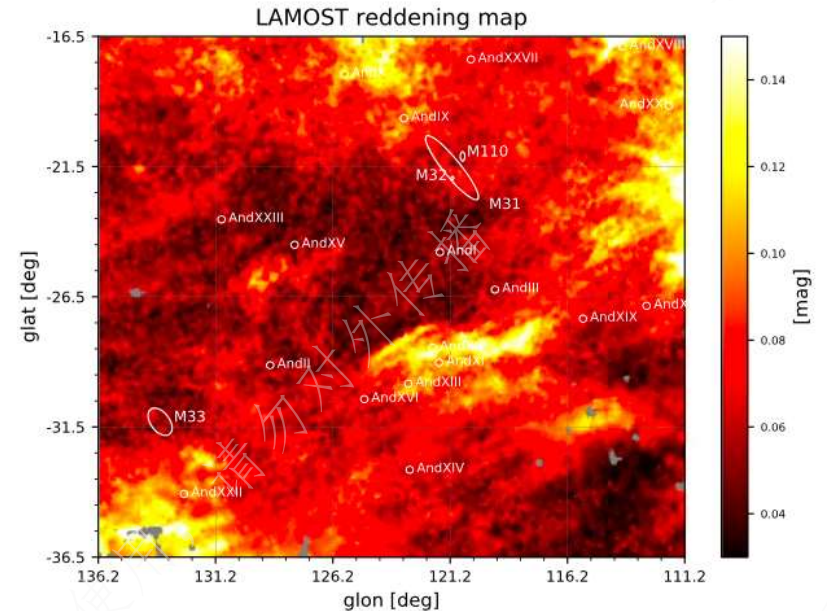
Background QSOs in the vicinity fields of M31/M33

~4000 QSOs
~100 PNs



Dust around M31

- LAMOST + Gaia
- 190,000 stars
- Reddening Map of MW
- Dust distribution of M31/M33



Pair of galaxies

- LAMOST + SDSS



Mass function of pairs

Interaction of galaxies: 150 kpc

Feng et al. 2019, ApJ

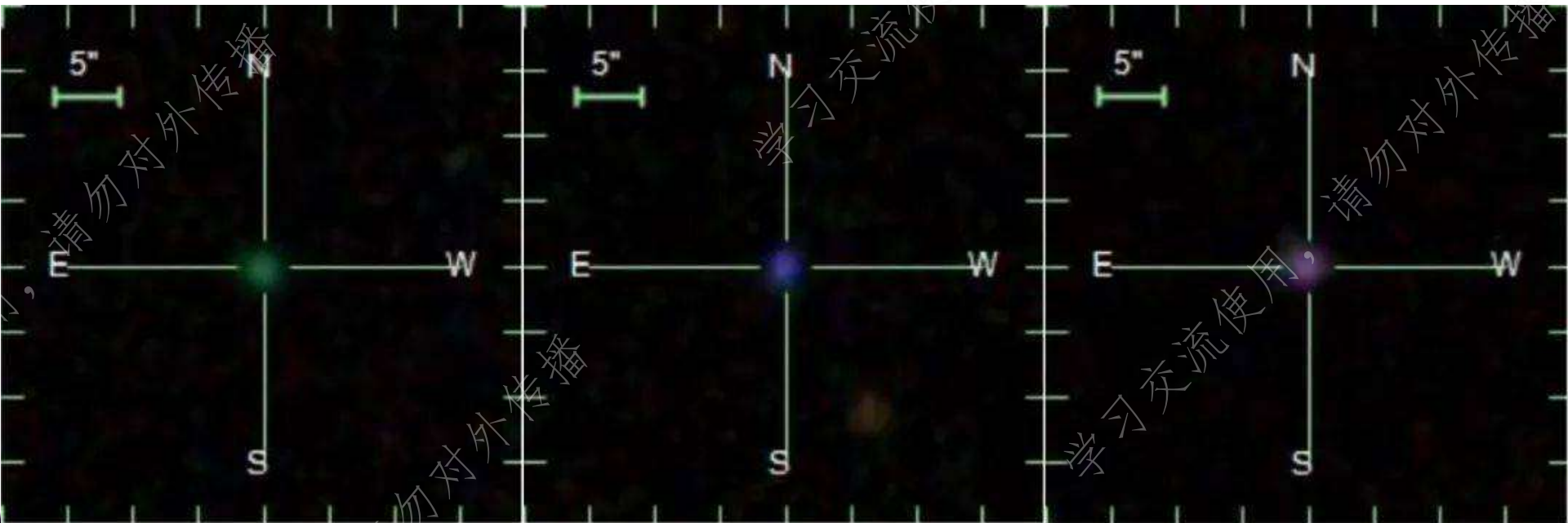


Compact galaxies:

“extragalactic fruit & vegetable garden”

1417 new discovery (before 800)

- **739 green pea**
- **270 blueberry**
- **388 purple grape**



Overview of the LAMOST survey in the first decade

Hongliang Yan,^{1,2} Haining Li,¹ Song Wang,¹ Weikai Zong,³ Haibo Yuan,³ Maosheng Xiang,⁴ Yang Huang,⁵ Jiwei Xie,^{6,7} Subo Dong,⁸ Hailong Yuan,¹ Shaolan Bi,³ Yaoquan Chu,⁹ Xiangqun Cui,^{10,11} Licai Deng,¹ Jianning Fu,³ Zhanwen Han,¹² Jinliang Hou,^{2,13} Guoping Li,^{10,11} Chao Liu,^{2,14} Jifeng Liu,^{1,2,15} Xiaowei Liu,⁵ Ali Luo,^{1,2} Jianrong Shi,^{1,2} Xuebing Wu,^{8,16} Haotong Zhang,¹ Gang Zhao,^{1,2} and Yongheng Zhao^{1,2,*}

*Correspondence: yzhao@nao.cas.cn

Received: April 23, 2021; Accepted: March 2, 2022; Published Online: March 8, 2022; <https://doi.org/10.1016/j.xinn.2022.100224>

© 2022 The Authors. This is an open access article under the CC BY-NC-ND license (<http://creativecommons.org/licenses/by-nc-nd/4.0/>).

GRAPHICAL ABSTRACT



PUBLIC SUMMARY

- LAMOST is an innovative telescope designed with both a large-aperture and a wide-FOV for astronomical spectroscopic survey
- LAMOST observed over 10 million objects in our Galaxy, and constructed the largest spectroscopic dataset
- LAMOST data changed the astrophysical viewpoint in the fields including stars, the Milky Way, exoplanets, and black holes

<https://arxiv.org/abs/2203.14300>

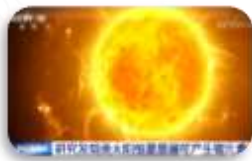
LAMOST亮点科研成果

• 富锂巨星系列成果



发现锂丰度最高的巨星

Yan et al. 2018, Nature Astronomy



类太阳恒星可以产生锂

Kumar et al. 2020, Nature Astronomy



富锂巨星真身探秘

Yan et al. 2021, Nature Astronomy

• 银河系结构研究



发现宇宙中金属含量最低的球状星团遗迹

Nicolas et al. 2022, Nature



揭示银河系早期形成和演化历史

Xiang et al. 2022, Nature

• 黑洞



发现最大质量恒星级黑洞

Liu et al. 2019, Nature

预期成果



Capability of LAMOST: $A\Omega = 247$

Existing and planned multi-object spectroscopic projects

Table 1: Existing and planned multi-object spectroscopic capabilities, with defining characteristics. These include wavelength range, field of view, etendue, the number of simultaneous spectra per field, the spectral resolution, the fraction of time the capability is in use, the image quality, and the discovery efficiency (defined in the text)

| Telescope/Instrument | D_{M1} (m) | Status | Available | λ (μm) | Ω (deg^2) | $A\Omega$ ($\text{m}^2 \text{deg}^2$) | N_{mos} | \mathcal{R} | f | IQ | $\log \eta$ |
|----------------------|-----------------------------|----------|-----------|--------------------------------|--------------------------------|--|-----------|---------------|-----|------|-------------|
| <i>Ground-Based</i> | | | | | | | | | | | |
| AAT/AAOmega | 3.9 | Existing | 1996 | 0.37–1.00 | 3.14 | 37.5 | 392 | 1000–17000 | 0.5 | 1.5 | 3.5 |
| SDSS | 2.5 | Existing | 2000 | 0.38–0.92 | 1.54 | 7.6 | 640 | 1800 | 1.0 | 1.4 | 3.6 |
| Keck/DEIMOS | 10.0 | Existing | 2002 | 0.41–1.10 | 0.023 | 1.8 | 150 | 2500–5500 | 0.4 | 0.7 | 2.1 |
| VLT/VIMOS | 8.2 | Existing | 2002 | 0.37–1.00 | 0.062 | 3.3 | 600 | 180–2500 | 0.2 | 0.8 | 2.9 |
| VLT/FLAMES | 8.2 | Existing | 2003 | 0.37–0.95 | 0.136 | 7.2 | 8–130 | 5600–25000 | 0.2 | 0.8 | 1.3–2.6 |
| MMT/Hectospec | 6.5 | Existing | 2004 | 0.36–0.92 | 0.79 | 26.1 | 240–300 | 1000–40000 | 0.2 | 1.0 | 2.6–2.7 |
| WIYN/Hydra | 3.5 | Existing | 2005 | 0.37–1.00 | 0.79 | 7.5 | 90 | 800–40000 | 0.2 | 0.8 | 2.4 |
| Magellan/IMACS | 6.5 | Existing | 2008 | 0.36–1.00 | 0.16 | 5.3 | 400 | 1100–16000 | 0.2 | 0.6 | 3.3 |
| SDSS/APOGEE | 2.5 | Existing | 2011 | 1.51–1.70 | 1.54 | 7.6 | 300 | 27000–31000 | 0.5 | 1.4 | 2.8 |
| Subaru/FMOS | 8.2 | Existing | 2012 | 0.8–1.8 | 0.20 | 10.4 | 400 | 600–2200 | 0.2 | 0.7 | 3.3 |
| LAMOST [†] | 4.0 | Existing | 2012 | 0.37–0.90 | 19.6 | 247 | 4000 | 1000–10000 | 1.0 | 3.0 | 5.1 |
| AAT/HERMES | 3.9 | Existing | 2013 | 4 windows | 3.14 | 37.5 | 392 | 28000 | 0.5 | 1.5 | 3.6 |
| Subaru/PFS | 8.2 | Planned | 2017 | 0.38–1.30 | 1.1 | 70 | 2400 | 1900–4500 | 0.3 | 0.7 | 5.0 |
| WHT/WEAVE | 4.2 | Planned | 2018 | 0.37–1.00 | 3.14 | 41 | ~1000 | 5000–20000 | 0.7 | 0.8 | 4.8 |
| Mayall/DESI | 4.0 | Planned | 2018 | 0.36–1.05 | 7.1 | 89 | 5000 | 3000–4800 | 0.5 | 1.5 | 5.1 |
| VLT/MOONS | 8.2 | Planned | 2018 | 0.8–1.8 | 0.14 | 7.3 | 1000 | 4000–20000 | 0.3 | 0.8 | 3.3 |
| VLT/4MOST | 4.1 | Planned | 2019 | 4 windows | 3.0 | 40 | 1500 | 3000–20000 | 1.0 | 0.8 | 5.1 |
| MSE | 10.0 | Planned | 2021 | 0.37–1.30 | 1.5 | 118 | 3200 | 2000 | 1.0 | 0.7 | 6.0 |
| | | | | 0.37–1.00 | | | 3200,800 | 6500,20000 | 1.0 | 0.7 | 5.4 |
| <i>Space-Based</i> | | | | | | | | | | | |
| Gaia | $2 \times (1.4 \times 0.5)$ | Existing | 2014 | 0.85–0.87 | all sky survey ($V < 17$) | | | 11500 | | | |
| Euclid | 1.2 | Planned | 2020 | 1.10–2.00 | 0.55 | 0.62 | | 250 | | | |
| WFIRST | 1.5 | Planned | 2025: | 1.10–2.00 | 0.5 | 0.89 | | 75–320 | | | |

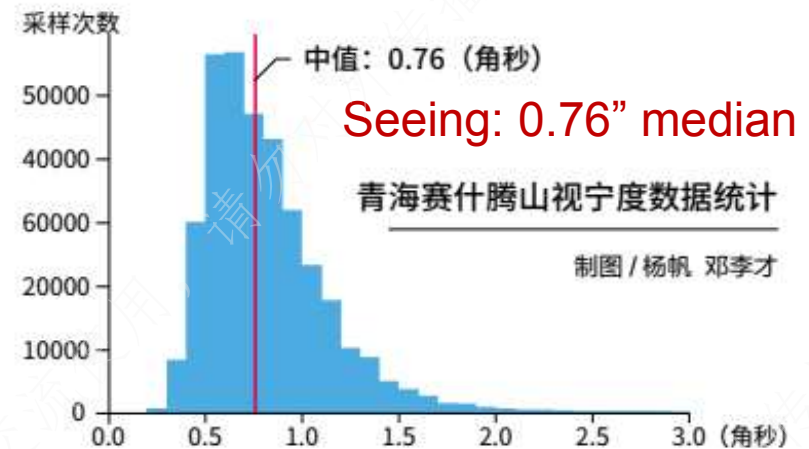
[†] – Also known as the Guo Shou Jing Telescope (GSJT).

A. McConnachie, R. Murowinski, D. Salmon, D. Simons, P. Côté c, 2014, SPIE

LAMOST II project

Site: Xinglong → Lenghu

- Mirrors: MA24 MB37
- Fibers: 4,000 → 12,000
- Limit mag.: 17.8m → 19.3m
- Spectra: 10 M → 100 M





学习交流使用，请勿对外传播

学习交流使用，请勿对外传播

学习交流使用，请勿对外传播

学习交流使用，请勿对外传播

Thank You !